AD-A188 861 BASELINE OBSERVING SYSTEM EXPERIMENTS USING THE AFGL GLOBAL DATA ASSIMILA..(U) ATMOSPHERIC AND ENVIRONMENTAL RESEARCH INC CAMBRIDGE MA J F LOUIS ET AL. 18 NOV 87 1/1

UNCLASSIFIED SCIENTIFIC-3 AFGL-TR-87-0327 F/G 4/2 NL

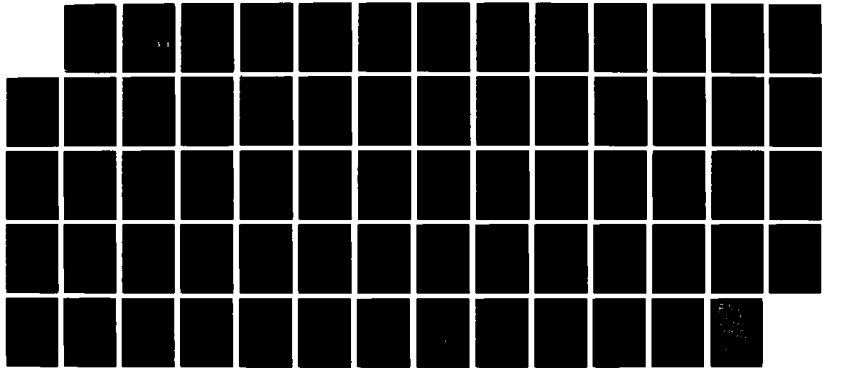

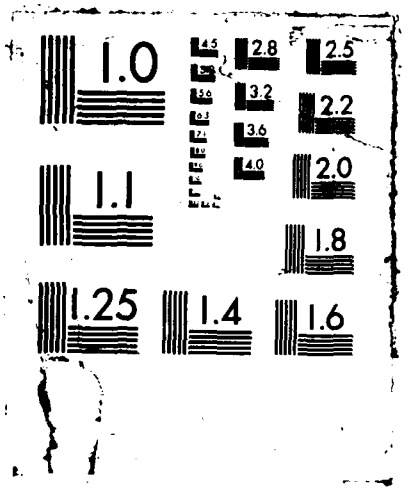
1.0
1.1
1.25
1.4
1.6
1.8
2.0
2.2
2.5
2.8
3.2
3.6
4.0
4.5

AFGL-TR-87-0327

BASELINE OBSERVING SYSTEM EXPERIMENTS USING THE AFGL GLOBAL DATA ASSIMILATION SYSTEM

J.-F. Louis, R.N. Hoffman, T. Nehrkorn, T. Baldwin and M. Mickelson

Atmospheric and Environmental Research, Inc.
840 Memorial Drive
Cambridge, MA 02139-3794

18 November 1987

Scientific Report No. 3

AIR FORCE GEOPHYSICS LABORATORY
AIR FORCE SYSTEMS COMMAND
UNITED STATES AIR FORCE
HANSCOM AFB, MASSACHUSETTS 01731

"This technical report has been reviewed and is approved for publication"

DONALD C. NORQUIST
Contract Manager

DONALD A. CHISHOLM
Branch Chief

FOR THE COMMANDER

ROBERT A. McCLATCHEY
Division Director

This document has been reviewed by the ESD Public Affairs Office (PA) and is releasable to the National Technical Information Service (NTIS).

Qualified requestors may obtain additional copies from the Defense Technical Information Center. All others should apply to the National Technical Information Service.

If your address has changed, or if you wish to be removed from the mailing list, or if the addressee is no longer employed by your organization, please notify AFGL/DAA, Hanscom AFB MA 01731-5000. This will assist us in maintaining a current mailing list.

Do not return copies of this report unless contractual obligations or notices on a specific document requires that it be returned.

Unclassified
SECURITY CLASSIFICATION OF THIS PAGE

REPORT DOCUMENTATION PAGE

1a. REPORT SECURITY CLASSIFICATION Unclassified	1b RESTRICTIVE MARKINGS
2a SECURITY CLASSIFICATION AUTHORITY	3 DISTRIBUTION / AVAILABILITY OF REPORT Approved for public release; distribution unlimited.
2b. DECLASSIFICATION / DOWNGRADING SCHEDULE	
4. PERFORMING ORGANIZATION REPORT NUMBER(S)	5 MONITORING ORGANIZATION REPORT NUMBER(S) AFGL-TR-87-0327
6a NAME OF PERFORMING ORGANIZATION Atmospheric and Environmental Research, Inc. 6b OFFICE SYMBOL (If applicable)	7a NAME OF MONITORING ORGANIZATION Air Force Geophysics Laboratory
6c. ADDRESS (City, State, and ZIP Code) Cambridge, MA 02139	7b ADDRESS (City, State, and ZIP Code) Hanscom AFB, MA 01731
8a. NAME OF FUNDING / SPONSORING ORGANIZATION Air Force Geophysics Laboratory 8b OFFICE SYMBOL (If applicable) AFGL/LY	9 PROCUREMENT INSTRUMENT IDENTIFICATION NUMBER F19628-86-C-0141
8c. ADDRESS (City, State, and ZIP Code) Hanscom AFB, MA 01731	10 SOURCE OF FUNDING NUMBERS

PROGRAM ELEMENT NO	PROJECT NO	TASK NO	WORK UNIT ACCESSION NO
61102F	6670	10	CB

11 TITLE (Include Security Classification)
Baseline Observing System Experiments Using the AFGL Global Data Assimilation System

12 PERSONAL AUTHOR(S)
J.-F. Louis, R.N. Hoffman, T. Nehrkorn, T. Baldwin and M. Mickelson

13a TYPE OF REPORT	13b TIME COVERED	14 DATE OF REPORT (Year, Month, Day)	15 PAGE COUNT
Scientific Report #3	FROM _____ TO _____	1987 November 18	64

16 SUPPLEMENTARY NOTATION

17 COSATI CODES			18 SUBJECT TERMS (Continue on reverse if necessary and identify by block number)
FIELD	GROUP	SUB-GROUP	Data Assimilation, Numerical Weather Prediction, Observing System Experiment.

19 ABSTRACT (Continue on reverse if necessary and identify by block number)

Four observing system experiments, have been performed with the AFGL data assimilation system. Each experiment includes one week of data assimilation during each special observing period of the FGGE year, and 3 four day forecasts, starting from the third, fifth and seventh day of the assimilation periods. The first experiment (STATSAT) provides a baseline for the other ones. It uses all the available level II-B FGGE data, except surface observations. Comparisons with the NMC level III-A analyses show that the AFGL system performs adequately. In the second experiment (NOSAT) all satellite data are removed from the data set. As expected the impact on the analysis is small in the Northern Hemisphere, but large in the Southern Hemisphere. This experiment provides a measure of the sensitivity that can be expected from future experiments in which different satellite retrieval techniques are tested. The third experiment (NOCON) was designed to test the degradation of the analyses when all conventional data are denied and only satellite data are used.

20 DISTRIBUTION / AVAILABILITY OF ABSTRACT	21 ABSTRACT SECURITY CLASSIFICATION	
☐ UNCLASSIFIED/UNLIMITED ☒ SAME AS RPT ☐ DTIC USERS	Unclassified	
22a NAME OF RESPONSIBLE INDIVIDUAL D. Norquist	22b TELEPHONE (Include Area Code) 617-377-2962	22c OFFICE SYMBOL AFGL/LYP

DD FORM 1473, 84 MAR 83 APR edition may be used until exhausted
All other editions are obsolete

SECURITY CLASSIFICATION OF THIS PAGE
Unclassified

19. ABSTRACT (continued)

Differences between this and the STATSAT experiment appear first over continental areas, but propagate quickly over the oceans, especially in the winter. The differences keep growing throughout the assimilation period. The forecasts from this experiment, especially the later forecasts, have little skill beyond 2 or 3 days. Finally a fourth experiment (NOCOR) examines the effect of denying conventional data only over a particular region (Europe and USSR). The effect is much smaller than in the NOCON experiment, even in the region where data was denied. Nevertheless the differences keep increasing during the assimilation period and some propagation of the differences across the Pacific and into North America is observed, especially in winter. The forecast errors, initially largest in the region of data denial, spread over the whole hemisphere in 3 or 4 days.

1. INTRODUCTION

To assess the impact of existing operational satellite retrieval data on global atmospheric analyses, we have performed four Observing System Experiments (OSEs). One additional experiment, making use of the experimental GLA physical retrievals is now underway and will be reported later. Each OSE consists of two one-week data assimilation runs, one each during Special Observing Period (SOP) I (February 1979) and SOP II (June 1979) of FGGE. The design and the evaluation of the OSEs are described in detail below. The observations used for these OSEs are those of the FGGE* II-b data set, which contains atmospheric soundings from pilot balloons and rawinsondes (at six-hour intervals), temperature and moisture soundings from the operational NOAA statistical satellite retrievals, cloud drift winds and surface data from land and ship stations as well as stationary and drifting buoys. (Not all of these data are used by the analysis system. Details are provided below.) The basic experiment for these tests is a STATSAT OSE in which all data are used in the analysis.

A great number of OSEs have been conducted with the FGGE data sets. A review of this subject, especially with regard to satellite data is given by Isaacs et al. (1986). The current general conclusions (Gilchrist, 1982) are that (1) satellite sounding data are vital to defining the large-scale structure of the atmosphere, and (2) the impact on forecast skill is positive but not very large by conventional measures, i.e., skill scores for continental areas. The OSEs reported here show to what degree these results are reproduced when a different data assimilation system, a different time period and different satellite retrievals are used.

To assess the impact of the operational statistical satellite retrievals, the results from the STATSAT experiment are compared with those from a NOSAT OSE, in which only conventional data from the FGGE II-b set of observations are used in the analysis. To determine to what degree satellite observations can replace conventional observations, we have repeated the STATSAT OSE twice, once without any conventional data (NOCON), and once with conventional data

---

*FGGE: First GARP Global Experiment

GARP: Global Atmospheric Research Program.

excluded over a specified continental region only (NOCOR). The results from these two OSEs are compared with each other, and with the STATSAT and NOSAT results.

1.1 Brief Review of Observing System Experiments

The quantitative assessment of the potential impact of a particular observing system on global Numerical Weather Prediction (NWP) requires a realistic simulation study. Such a study can help to optimize the design of a planned observing system by exploring the sensitivity of the resulting impact to possible design tradeoffs. It is then called an observing systems simulation experiment (OSSE). Studies utilizing real data, termed observing system experiments, may also be used to evaluate the usefulness of a particular actual observing system, either using a degraded set of observations or a different data treatment. In both OSSEs and OSEs, parallel 4D assimilation and forecast runs, made with and without a particular observing system, are compared and evaluated objectively and subjectively. In a similar vein, in impact tests of the model formulation, parallel forecast ensembles made with two different resolutions, finite difference methods or parameterizations of a physical process, may be used to quantify a model sensitivity.

There are a number of design and interpretation issues which must be considered in our discussion of impact studies. Gilchrist (1982) discussed the major concerns involving OSEs. His main points can be summarized as follows. (1) When the satellite soundings used are obtained statistically, one must bear in mind that the situations when these extra observations are expected to be important are not necessarily the "normal" situations which made up the bulk of the data base used to develop the statistical retrievals. (2) The analysis systems have usually been developed and tuned for conventional data. In particular, the statistical properties of the satellite observations - low vertical resolution, low horizontal variance, biases - were not properly taken into account. Phillips (1976) analyzed this point in detail. It is true that over oceans these statistics are difficult to estimate; just as the small ocean radiosonde data base makes it hard to develop statistical retrievals, it also makes it hard to evaluate statistical retrievals. (3) The sample of cases examined is usually small and may not be representative. Also, predictability varies from case to case; some cases are

relatively insensitive to small changes in initial conditions. (4) Different models will accept or reject a particular type of data to different degrees. Impact depends on the specific model used. For example, Atlas et al. (1982a) found that satellite data produced a larger positive impact when used in a model with higher resolution. (5) Quality control is necessary in any system; there may be a substantial impact on a particular case due to the inclusion or exclusion of a particular radiosonde report which is borderline, i.e. which deviates enough from the first guess to be close to the rejection criterion. In recent intercomparisons of the response of NWP systems to the FGGE data base, some significant differences could be traced to quality control procedures (Hollingsworth et al. 1985). Gutowski and Hoffman (1985) have proposed a procedure to lessen this sensitivity by adjusting the weight given to suspect observations.

1.2 Purpose of the Present Experiments

The purpose of the experiments reported here is three-fold: to evaluate the impact of satellite data on the AFGL data assimilation system, to assess the effect of denying part or all of the conventional data, and to test the quality of the AFGL system. The first and last goals are in fact closely linked. A complete evaluation of the impact of satellite data on NWP would require resources well beyond those available to this project. This more limited work will show how this particular assimilation system handles a particular set of satellite data, in a small number of cases. Hence it is likely to tell us more about the performance of the data assimilation system than the usefulness of satellite data in NWP. We may be able to see whether our results are consistent with those of other, more extensive studies, but we should be cautious of drawing any definite conclusions on the basis of the small sample that will be available to us.

While performing the assimilation experiments described below, we have determined that the analysis system is performing reasonably. The main validation of the performance of the assimilation system comes from the results of the STATSAT OSE described below. The input data for this experiment closely parallels that used by NMC to produce its FGGE Level III-a analyses. Comparison of NMC III-a analyses with those from the STATSAT experiment confirms that the assimilation system is performing adequately except for

some large differences at the surface. (As noted below, no use is made of surface observations in the analysis.)

To test the sensitivity of the assimilation system to satellite data, a second experiment, called NOSAT, is performed, with all satellite data removed. The extent of the usefulness of satellite data has been shown by previous research, but this test gives us an idea of the kind of sensitivity that can be expected from other experiments, to be performed later, in which different satellite retrieval techniques are compared.

In the last two experiments, the effect of denying conventional data is studied. First, in the NOCON experiment, all the conventional data are removed from the data set. This gives an indication as to what extent a purely space-based system can satisfy the data requirements for NWP, were conventional data to become unavailable. Finally, a less drastic situation is examined in experiment NOCOR, in which conventional data are denied over a region of the globe, specifically over Europe and the USSR.

1.3 The AFGL Forecast/Analysis System

The series of 4D data assimilation experiments described here make use of existing computer codes and data bases at AFGL. The assimilation cycle consists of a sequence of three major steps: analysis, normal mode initialization, and forward integration of the initialized state to the next analysis time. Some pre-/post-processing of the data may occur between the major steps. An entire assimilation run is a repetition of this sequence until an initialized analysis is obtained at the ending time.

Optimal interpolation (OI) provides the mechanism for obtaining regularly gridded initial conditions, i.e., analyses, from incomplete, irregularly spaced data. The AFGL Statistical Analysis Program (ASAP), is actually composed of four individual programs. The ASAP OI was developed by SASC for AFGL/LYP and is documented in a series of reports by Norquist and others (Norquist, 1982b, 1983, 1984, 1986; Halberstam et al., 1984). The ASAP OI is based on the NMC assimilation system, as reported in the literature and in personal communications; this system was thoroughly redesigned and recoded by SASC personnel. According to Norquist (1986), ASAP was developed originally from the 1979 multivariate OI procedure as described by Bergman (1979) and by McPherson et al. (1979), with some assistance from NMC personnel (Morone,

1983, private communication). The ASAP OI is a multivariate analysis of height and wind components and a univariate analysis of relative humidity, both in model sigma layers. The equations for these weights as well as the computation of the horizontal and vertical correlation functions follow Bergman (1979). The analysis error evolves according to simple rules (Norquist, 1986). The great circle distance method for correlation functions equatorward of 70° latitude is included as described by Dey and Morone (1985) without changing the Bergman formulation (including map factor) for latitudes poleward of 70° latitude.

Data used by the height-wind analysis include Type 1 observations (radiosondes, pibals, etc.), Type 2 observations (aircraft), Type 4 observations (satellite-retrieved temperatures or thicknesses) and Type 6 observations (cloud drift winds (CDWs)). The Type 3 surface observations are not used at all. This implies that satellite "heights" are anchored only by the 6 h forecast in regions where radiosondes are absent or denied. The moisture analysis used in the experiments reported here uses only Type 1 data. Consequently, during the NOCON experiment there was no moisture analysis. In all experiments, except for the three-day preliminary assimilations, the CDW data (Type 6 data) were combined (i.e., locally averaged) into super-obs. There are two principal reasons for doing this: First, to limit the total number of observations, so that computer memory restrictions are not exceeded, and second, the CDW errors are strongly correlated horizontally because the main error source is due to height assignment (McPherson, 1984). Because of new quality control codes inserted by the NASA/NMC Special Effort the quality control translation tables for Type 6 data in ASAP were altered. The only other change made to ASAP for these experiments was to alter the satellite height observational error statistics (Table 1).

Table 1

Observational error standard deviations (m) used for satellite and radiosonde heights. Note that we use different values for February and June. The STATSAT and NOSAT experiments were already underway before the most up-to-date values were available. For comparison, satellite height observational standard deviations equivalent to the temperature observational error statistics used by NMC in 1979 are included. The radiosonde errors are from Dey and Morone (1983) and the satellite errors are from Norquist (1986; pers. comm., 1987). The NMC-1979 satellite errors are calculated hydrostatically from the standard deviations of temperature error from McPherson et al. (1979), the vertical correlation of temperature error from Bergman (1979) and an assumed height error at 1000 mb uncorrelated with the temperature errors.

Pressure (mb)	Radiosonde	February NOSAT/STATSAT	February NOCON/NOCOR	June NOSAT/STATSAT	June NOCON/NOCOR	NMC (1979)
1000	7.0	9.75	9.75	9.75	9.75	9.75
850	8.0	23.67	14.94	25.39	12.53	12.45
700	8.6	35.19	19.56	32.92	20.87	18.66
500	12.1	49.27	27.88	31.12	26.76	28.48
400	14.9	70.07	34.88	53.61	32.74	33.51
300	18.8	97.87	43.51	68.66	40.32	39.40
250	25.4	95.09	46.59	65.47	43.60	42.14
200	27.7	98.32	47.40	57.34	44.66	46.46
150	32.4	90.82	43.80	48.44	46.51	53.37
100	39.4	75.95	56.60	54.28	54.28	58.77
70	50.3	61.32	61.30	53.61	53.61	61.76
50	59.3	67.91	67.91	64.75	64.75	64.85

The normal mode initialization (NMI) is a part of the forecasting system which adjusts the initial data in such a way that undesirable gravity waves do not grow in the forecast. The AFGL NMI was developed by SASC, based on the NMC NMI. The NMC NMI is described by Ballish (1980). The AFGL version, much of which is taken intact from the NMC codes, is discussed by Norquist (1982a) and Tung (1983). The NMI program is actually two programs, one which calculates the normal modes (i.e., eigensolutions of the discrete linearized model equations) and one which performs two iterations of the Machenhauer initialization procedure which sets the time tendencies of the gravity modes approximately to zero. We altered the Machenhauer initialization procedure to make use of the tendencies calculated by the AFGL GSM. To accomplish this we altered the GSM to write out tendencies if desired. We then developed a program to add in the linear tendency terms, not explicitly calculated by the GSM and perform a single Machenhauer projection. The GSM tendency and Machenhauer projection calculations are repeated twice to obtain a complete initialization. The NMC Machenhauer projection codes were used with no alterations. The procedure was tested by temporarily making small changes to the AFGL GSM so that its physical constants and parameterizations would agree with the NMC tendency calculation used in the previous NMI. Extremely good agreement was obtained.

The AFGL global spectral model (GSM) is based on the NMC GSM designed by Sela (1980). For the version used here, the physics routines are taken almost intact from NMC (circa 1983). The hydrodynamics, i.e., the nonadiabatic, inviscid dynamics including vertical and horizontal advection, time stepping, and transformations between spectral and physical space, were completely redesigned, as documented by Brenner et al. (1982, 1984). As mentioned above, there are only minor differences between the AFGL and NMC GSMs, at least as far as the calculation of the dry tendencies.

There are a number of parameters in the assimilation cycle codes that can be adjusted. Typically, the parameters have the same values as used by Brenner et al. (1984) and Halberstam et al. (1984). Briefly, the spectral resolution of the forecast model is rhomboidal 30. The Gaussian grid of the forecast model (analysis) contains 76 x 96 (62 x 64) latitude longitude points. There are 12 layers, the first (top) 5 of which have no moisture. The sigma interfaces are at 0.00, 0.05, 0.10, 0.15, 0.20, 0.25, 0.30, 0.35, 0.50, 0.65, 0.80, 0.925, and 1.00. The time scheme used is centered semi-

implicit with a time step of 17.25 minutes and a Robert time filter is applied with a constant of 0.04. A spectral diffusion coefficient of 6×10^{15} $m^{-4}s^{-1}$ ($6 \times 10^{16} m^{-4}s^{-1}$) is applied during the forecasts (assimilation cycle) to all prognostic variables except for moisture. In the NMI, two Machenauer iterations are applied to modes for the four largest equivalent depths which have periods less than or equal to 48 h.

Except for the correction of a few minor errors discovered by scientists at AFGL/LYP during the course of the contract, no substantive changes were made to the assimilation system other than those noted. Some additional diagnostic capabilities were added. These additions include a file of rejected observations from the ASAP OI and the calculation of divergence, vorticity and vertical velocity all in pressure coordinates, within the post-processor.

1.4 Methodology

Each impact test consists of assimilation runs for two 7-day periods during the FGGE SOPs: February 8 through 15, 1979, and June 17 through 24, 1979. The SOP I and SOP II periods are treated in the same fashion.[1] Each assimilation run consists of a series of assimilation cycles, and each cycle in turn is made up of a 6-hour forecast that serves as a first guess for the analysis, an optimum interpolation analysis which combines the first guess fields with the observations, and a nonlinear normal mode initialization of the analysis. The initialized analysis is the starting point for the next 6-hour forecast, which is then used as the first guess of the subsequent assimilation cycle. The forecast model used for the 6-hour forecast is the full GSM. The same model[2] is also used to produce 96 h forecasts starting from days 3, 5, and 7 of the assimilation runs.

The initial conditions for the first assimilation cycle of each assimilation run starting on the same date is the same for all OSEs. One could use an initialized III-a or III-b analysis for that purpose, but that would have

[1] Observing error standard deviations for satellite heights are specified differently for each period, however (see Table 1).

[2] Different values are used for the diffusion coefficients.

the disadvantage that, during the initial period of each OSE, the system would be undergoing adjustments because the level III analyses are not entirely compatible with the assimilation system used in the OSE. To avoid that complication, we have performed a 3-day assimilation run once for each SOP period, starting from an initialized level III NMC analysis, with the full FGGE data base (i.e., similar to the STATSAT OSE except that the CDWs were not super-obbed). The final initialized results from these two "spin-up" assimilation runs then serve as the starting point for all OSEs reported here.

Independent analyses for the same time period, performed by NMC using level II-a data, provide some benchmarks for the interpretation of analysis skill and characteristics. We directly compare our analyses with the corresponding level III analyses, computing mean and RMS differences. In addition, the data fitting characteristics, smoothness, and meteorological realism of the different analyses are compared with each other. Finally, a measure of the quality of the analyses is given by the skill of forecasts made from them. We evaluate these forecasts against the independent level III analyses of NMC.

2. STATSAT EXPERIMENT

The first experiment, named STATSAT, uses all the available upper air data in the FGGE dataset. This includes satellite temperature soundings provided by NESDIS, but not satellite moisture soundings. The retrieval method used statistical regressions between temperature profiles and measured radiances. This is the same dataset as was used by ECMWF for their FGGE analyses, and essentially the same as was used by NMC for their operational analyses. The differences that can be observed between the STATSAT analyses and the NMC or ECMWF analyses are thus mainly due to differences in the analysis/forecasting systems, including differences in the data selection algorithm. We will mainly compare STATSAT and NMC uninitialized analyses. Except for differences at the lower levels, which may be due to the fact that the AFGL analysis system does not use surface observations, the STATSAT and NMC analyses appear to be quite similar at first glance. A more detailed examination reveals differences which can, occasionally, be quite substantial and synoptically significant.

February

In the Northern Hemisphere winter, the 500 mb height differences reach 150 to 200 m. Some regions appear more prone to large differences. The most striking differences are associated with a deep, quasi-stationary trough in the Gulf of Alaska. The shape and phase of this trough are often different. The main baroclinic zone in the trough tends to be further south in the STATSAT analyses, and the small waves that are superimposed on the main trough (and the following broad ridge over the Rockies) have little in common (Fig. 1).

In the Eastern Pacific, off the coast of Central America, the NMC analyses show a broad region of low pressure which seems to be absent in the STATSAT analyses. Differences in the phase and shape of the flow are also evident over northern Europe throughout the winter period.

These differences are even more striking at 1000 mb. In fact, the STATSAT and NMC analyses of the 1000 mb flow can be remarkably different. For example, on February 8, 12Z, the NMC analysis shows the flow to be parallel to the northwest coast of North America, while in the STATSAT analysis the flow crosses the coast (Fig. 2).

On 10 February 00 GMT, the low over Finland has a depth of -174 m in the NMC analysis, but only -84 m in the STATSAT analysis (Fig. 3). The center of the low is also displaced, producing quite a different flow over the Scandinavian peninsula.

The differences between STATSAT and NMC analyses in February are larger in the southern hemisphere, frequently exceeding 250 m, both at 500 and 1000 mb. The flow generally appears slightly more zonal, especially at 1000 mb, and the gradients somewhat weaker in the STATSAT analyses. A striking difference is the absence, in the STATSAT analysis of February 13, of an intense low in the south of the Indian Ocean (Fig. 4). This feature is present both in the NMC and in the ECMWF analyses, and seems to have evolved from a small scale tropical storm. There is only the hint of a trough in the STATSAT analysis.

Over the Antarctic continent during the whole February period, the 500 mb STATSAT analysis is about 200 m higher than the NMC analysis. The differences are also large at 1000 mb in that region, but not so systematic.

Some differences are associated with orographic features. The NMC analyses have a localized stationary high along the coast of Chili, upwind of the Andies, more pronounced at 00Z than at 12Z. They also show odd, persistent small scale features over the Red Sea, Gulf of Arabia and Caspian Sea (more apparent in the difference fields). Both are absent in the STATSAT analyses.

We have examined the relative humidity fields mostly at 850 mb over the north Atlantic region. The differences between the STATSAT and NMC analyses are fairly large, often exceeding 50%. They are often related to differences in the synoptic patterns. The STATSAT relative humidity analyses tend to show more small scale structure over North America, and to be drier over the subtropical Atlantic, near the African coast (Fig. 5).

June

In June, the 500 mb height differences are somewhat smaller in the Northern Hemisphere, rarely exceeding 100 m, as can be expected from the weaker summer circulation. One interesting exception is on 21 June, 00 GMT. In the STATSAT analysis the trough near the east coast of North America extends east into the Atlantic, while the NMC analysis has its maximum high there (Fig. 6).

The circular pattern in the difference map suggests that the anomaly may be due to a different data selection. An examination of the data file revealed that, on that day, a radiosounding was taken by ship UZGX at 36.3N, 57.4W, very close to the center of the difference pattern. The observed 500 mb height was 5840 m. The STATSAT analyzed height is 5810 m, whereas the NMC height is 6000 m, much further from the observed value. In this case, the ECMWF analysis falls between the STATSAT and NMC fields, with a height of about 5850 m. Thus it appears that, either this sounding was not available to the NMC operational analysis system, or it rejected the information, while both the STATSAT and ECMWF took it into account.

At 1000 mb, the differences are also fairly small. There is a tendency for the STATSAT analyses to be higher than the NMC analyses over the continents, and lower over the oceans (Fig. 7). Essentially, the STATSAT oceanic highs are not as strong as in the NMC analyses.

Over Antarctica, the June STATSAT analyses are systematically higher than the NMC analyses, by up to 400 m at 500 mb (Fig. 8). This means that the polar vortex is less intense in the STATSAT analyses than in the NMC ones. In addition, large differences in the phase and amplitude of the waves make the two southern hemisphere analyses noticeably different (Fig.9).

Forecasts.

The first STATSAT forecasts of the series can be evaluated either against the NMC analyses, or against the STATSAT analyses themselves. The later forecasts can only be compared to the NMC analyses since STATSAT analyses are not available beyond February 15 or June 24. Hence we will mostly compare the forecasts to the NMC analyses and, unless otherwise specified, we will write "forecast errors" for the differences between the STATSAT forecasts and the NMC analyses.

At the beginning, the forecast errors are mainly related to differences between the initial (STATSAT) analysis and the NMC data. For example, in the 12 hr forecast from February 11, 00Z, the widespread negative errors in the eastern Pacific and western Atlantic (Fig. 10) are clearly amplifications of similar negative differences in the analyses (compare to Fig. 1(c)).

The evolution of differences during the assimilation cycle and forecasts is displayed in Fig. 11. The dot-dashed line shows the evolution of the root mean square (rms) difference between the STATSAT and the NMC 500 mb height analyses. The solid lines are the rms STATSAT forecast errors (forecast-NMC analysis), also at 500 mb. The first and last forecasts of the series are shown. Finally, the dotted line is the rms difference between the STATSAT forecast and the corresponding STATSAT analysis. Each hemisphere and season is plotted separately. These plots confirm what has been found from the examination of the maps. The analysis differences are larger in the Southern Hemisphere than in the Northern Hemisphere, and larger in the winter than in the summer. The forecast errors grow somewhat more slowly in the summer than in the winter. After 48 hours, in the Northern Hemisphere, the rms forecast errors become nearly independent of the reference analysis. In the Southern Hemisphere, by contrast, the STATSAT forecasts remain closer to the STATSAT analyses than to the NMC analyses throughout the length of the forecasts

Systematically, all the STATSAT forecasts are drier than the NMC analyses over the sub-tropical Atlantic (between 10 and 30N). Since few data exist in that region, it is not clear what the truth is. The STATSAT analyses are drier too. These differences may be due to some differences in the physical parameterizations, perhaps the Kuo convection, or to differences in the prescribed sea surface temperature.

3. NOSAT EXPERIMENT

In the NOSAT assimilation experiment all satellite data are removed from the dataset. Only conventional data are used. Thus we expect differences between the NOSAT and STATSAT analyses mainly over the oceans and the southern hemisphere. Over the Northern Hemisphere continents, where conventional data are numerous, differences are expected only to the extent that the first guess, which advects the errors from the data-sparse regions, influences the analyses.

February

As can be seen in Fig. 12, the differences between the two analyses grow during the period. In February, in the Northern Hemisphere, the differences remain fairly small, rarely exceeding 100 m, and reach their maximum amplitude after about 4 days of data assimilation. The largest differences occur over the oceans, but some propagation onto the continents can be observed, especially over North America (Fig. 13).

When compared to the NMC analyses, the NOSAT fields exhibit similar kinds of differences as the STATSAT fields do, but usually somewhat larger. For example, there is the same tendency to spread the baroclinic zone further south in the Pacific trough, but now this tendency can also be seen in the Atlantic (Fig. 14). Usually, the STATSAT analyses are closer to the NOSAT analyses in the Northern Hemisphere than to the NMC analyses. There are a few exceptions: on February 14, the NOSAT analysis has a small ridge over the bay of Biscay, which is absent in the STATSAT and NMC analyses, and the STATSAT low near Kamchatka is similar to the NMC one, while it is split in the NOSAT analysis.

Since the satellite moisture data included in the FGGE dataset are not used, the differences in relative humidity between the NOSAT and STATSAT

analyses are due only to the different temperature fields and are small throughout the assimilation period.

The Southern Hemisphere differences between the NOSAT and STATSAT analyses keep growing throughout the assimilation period, reaching values of 300 m on February 15. They do stay small over the land masses, however, even over Antarctica (Fig. 15). The deep low analyzed by NMC in the Indian Ocean around February 13 is also completely absent from the NOSAT analysis. The flow is also noticeably more zonal than in the NMC analyses, more so than the STATSAT analyses. For example, on February 9, 00Z, all highs of the NMC analysis are higher and most lows are lower than in the NOSAT analysis, indicating that the NOSAT waves have smaller amplitudes.

June

In June, the Northern Hemisphere analyses remain very similar throughout the assimilation period, with height differences barely reaching 50 m. In the southern hemisphere, on the other hand, differences already exceed 100 m after the first day of assimilation, and soon reach more than 300 m. By June 20 the two analyses begin to diverge, with the STATSAT fields remaining much closer to the NMC analyses than to the NOSAT analyses. This is especially true southwest of Australia, where on 22 June the NOSAT analysis shows a ridge where both the STATSAT and NMC analyses have a trough (Fig. 16). After that point the STATSAT and NOSAT analyses have little in common. Most of the differences between the two analyses occur in the regions where there are no radiosounding stations. This can be seen on Fig. 17, where the station positions are indicated on the 500 mb difference map for June 21. Only at two stations does the difference reach or exceed 80 m: Marion Island (46.9S, 37.9E) and Gough Island (40.3S, 8.9W). Table 2 shows that, in both cases, the STATSAT analysis is closer to the observed value than the NOSAT analysis.

We checked the rejected data files and found that both height and wind data at Gough Island were rejected by the gross check of the NOSAT analysis, meaning that the data were considered too far from the first guess to be used. At Marion Island the NOSAT analysis rejected the wind data. In the STATSAT experiment all these data were retained.

Table 2

Height of the 500 mb surface at 2 Southern Hemisphere island stations.

	STATSAT	NOSAT	Observed
Marion Island	5540	5450	5590
Gough Island	5520	5600	5520

Toward the end of the assimilation period, some rather large differences begin to appear even in regions where radiosonde data are available. On June 24 (Fig. 18), large differences can be seen in the 500 mb fields near New Zealand, despite three existing radiosonde measurements. Table 3, which gives the observed and analyzed 500 mb heights, again shows that the STATSAT analysis is closer to the observations than the NOSAT analysis. The Macquarie Island data was rejected by the NOSAT analysis. This suggests that, at least in the Southern Hemisphere, satellite data are beneficial even where conventional data exist.

Table 3

Height of the 500 mb surface at 3 stations.

	STATSAT	NOSAT	Observed
Christchurch	5690	5540	5710
Invercargill	5650	5440	5670
Macquarie Isl.	5280	5180	5240

Forecasts

As in the case of the STATSAT forecasts, the differences between the NOSAT forecasts and the NMC analyses can, in the short range, often be traced to differences in the initial analyses. In the Northern Hemisphere, the NOSAT

forecasts are quite similar to the STATSAT forecasts. In fact, comparing Fig. 19 to Fig. 11, the Northern Hemisphere rms differences for the NOSAT experiment are almost indistinguishable from those for the STATSAT experiment, especially in the summer. The 96 hr 500 mb and the 72 hr 100 mb forecasts would generally be considered poor forecasts.

In the Southern Hemisphere, the NOSAT forecasts quickly differ from the STATSAT forecasts. As early as 72 hrs into the forecasts, the Southern Hemisphere fields are so different from the NMC analyses that they can be considered useless. By that time, the range of the errors is larger than the range of variation of the fields. Compared to the NOSAT analyses, however, these same forecasts remain quite "good" (i.e. similar to the analyses), sometimes up to 96 hrs. A typical case is the 48 hr Southern Hemisphere forecast from June 20, 00Z (Fig. 20). Even though on June 20 the two analyses are fairly similar, by June 22 the NOSAT analysis shows a strong ridge between Africa and Australia, while a trough remains in the STATSAT analysis, as well as in the NMC and ECMWF analyses. A very similar ridge develops in the 48 hr NOSAT forecast from June 20. Without the satellite data, the NOSAT assimilation is dominated in the Southern Hemisphere by the forecast.

4. NOCON EXPERIMENT

The NOCON experiment is designed to study the effect of a completely space-based observing system. All the conventional data are removed from the FGGE dataset. Only satellite data are used, but these are used over the continents as well as over the oceans, in contrast to the STATSAT experiments in which satellite data are used only over the oceans. Obviously the biggest effect is expected over the continents. However, it should be remembered that the available satellite soundings only provide temperatures or, equivalently, thicknesses. The height of a reference pressure level is also needed to compute the height of all the pressure levels. In our experiments the reference height (height of the lowest standard pressure level above the ground) is provided by the forecast first guess. In the NOCON experiment we expect that errors in this forecast will eventually corrupt the entire analysis.

February

In the Northern Hemisphere, the 500 mb differences between the NOCON analyses and the STATSAT analyses keep growing throughout the assimilation period. On February 13, the fields are noticeably different over northern Europe (Fig. 21), and by February 14 the differences are large throughout the Northern Hemisphere. On February 15 the differences reach more than 350 m at one point (Fig. 22). They do not exceed 100 m over North America, however. A similar behavior is observed at 1000 mb, also with a somewhat smaller amplitude in Eurasia (250 m), and larger in North America (150 m). One week of data assimilation is not sufficient to determine how large the differences between the analyses of this space-based system and the STATSAT analyses would eventually become.

While the overall patterns of the relative humidity field are fairly similar in the two analyses, large small-scale differences abound (Fig. 23).

In the Southern Hemisphere the differences remain much smaller than in the Northern Hemisphere, except over the polar cap where the 500 mb height difference reaches 200 m on February 15.

June

In the Northern Hemisphere, the June NOCON analyses differ from the STATSAT analyses by a smaller amount than in February, and the differences stay mostly confined to the continental areas (Fig. 24). The differences are very similar at 500 and 1000 mb. In the Southern Hemisphere, on the other hand, the difference pattern is striking. After one day of assimilation (June 18), an area of negative difference has appeared, which covers almost exactly the Antarctic continent (Fig. 25). This pattern grows in strength and area until, on June 24, it reaches almost 450 m. Nearly the opposite occurs at 1000 mb, with the difference field being mostly positive over Antarctica. Obviously, since the surface of the continent is far above the 1000 mb level, this positive difference may merely indicate a different lapse rate above the surface in the two analyses.

Forecasts

All the NOCON forecasts behave in a similar fashion, compared to the STATSAT forecasts. We will take the forecast from June 20 as an example. At the beginning of the forecast the NOCON 500 mb forecast errors (NOCON forecast minus NMC analysis) are similar to the STATSAT forecast errors, but slightly larger. The two forecasts start diverging after 48 hrs in the Northern Hemisphere, with phase differences noticeable over North America and Scandinavia. The differences keep growing and, at 96 hrs, the two forecasts, while still keeping a family resemblance, are different in all details (Fig. 26).

At 1000 mb the differences appear sooner. Already at 24 hrs differences are visible over North America. At 48 hrs a low present over Canada in the STATSAT forecast is absent in the NOCON forecast. By 72 hrs, the two forecasts are quite different.

The Southern Hemisphere forecasts are more similar, starting to diverge only after 72 hrs, except over Antarctica where differences in the 500 mb fields are apparent already after 24 hrs.

Since no data was used in the NOCON humidity analyses, it is not surprising that the NOCON and STATSAT relative humidity forecasts are very different.

An interesting insight in the difference between the STATSAT and NOCON analyses is provided by Fig. 27 and Table 4, where two analyses and two 4-day forecasts for the same day are compared. It can be seen that the NOCON 1000 mb analyses are as different from the STATSAT analyses as the 4-day forecasts are from their verifying analyses. Figs. 28 and 29 summarize the results of our NOCON-STATSAT and NOCON-NMC comparisons.

Table 4

Root mean square differences between 1000 mb analyses and 4-day forecasts for 00 GMT 15 February 1979.

	ANALYSES		FORECASTS	
	NOCON	STATSAT	NOCON	STATSAT
FORECASTS				
STATSAT	56.8	62.5	48.1	0.0
NOCON	49.4	66.7	0.0	
ANALYSES				
STATSAT	51.2	0.0		
NOCON	0.0			

5. NOCOR EXPERIMENT

In the NOCOR experiment we investigated the effect of denying conventional data in a limited region of the globe. The area chosen covered Europe and USSR, as indicated on Fig. 30. Only satellite data were used there. Another difference with the STATSAT experiment is that satellite data were used over all continental areas as well as over the oceans.

February

The differences between the NOCOR and STATSAT analyses keep growing during the whole assimilation period in the region where the data was denied. Over Siberia the 500 mb height differences reach more than 200 m. At the same time, differences propagate across the Pacific ocean, reaching the west coast of North America in about four days. Fig. 31 shows the evolution of the difference patterns during the data assimilation period. Comparing Fig. 30(c) with Fig. 22, it can be seen that, in the Europe/USSR region, the NOCOR analysis is closer to the STATSAT analysis than the NOCON analysis is, even though they both used the same data in that region. This indicates that, in

the NOCOR analysis, the better quality of the first guess slows the growth of differences. As in the NOCON experiment, one week of data assimilation may not be sufficient to determine the asymptotic behavior of this observing system.

At 1000 mb the differences between the NOCOR and STATSAT analyses stay somewhat smaller than at 500 mb, barely exceeding 120 m, and no longer appear to grow after 13 February. From a synoptic point of view, the 1000 mb NOCOR and STATSAT analyses are fairly similar. A typical example is shown in Fig. 31. The pressure gradients over northern and eastern Europe are different, and there are some significant phase differences, but the overall patterns are similar.

The differences in the relative humidity field are mostly confined to the region where data were denied. The differences tend to be of small scale, but of large amplitude, often exceeding 60%.

June

In the summer, the differences between the NOCOR and the STATSAT analyses stay fairly small, and their amplitude no longer increases after about 3 days of assimilation. Some propagation of the differences into the Pacific area is observed. The amplitude and phase of the fast-moving low East of Kamchatka is modified, resulting in differences of up to 120 m for the 500 mb height in that region of the Pacific on 22 June (Fig. 32)

Forecasts

The differences between the NOCOR and STATSAT forecasts are in general not very large. They are larger in winter than in summer as expected from the more intense winter circulation. The propagation of the differences across the Pacific is also quicker in winter than in summer. In the first forecast of the series (starting February 11), differences of 90 m at 500 mb appear on the west coast of north America at 24 hrs. By 72 hrs, differences of about equal magnitude can be seen at all longitudes (Fig. 33). In summer, on the other hand, the differences remain smaller in the western half of the hemisphere than in the eastern half throughout the forecast.

In the same way as the analyses become more different as the assimilation

cycles progress, the forecasts differences are larger for those starting from the end of the assimilation periods. For example, the differences between the NOCOR forecast from February 15 and the STATSAT forecast starting on the same date are about as large as the STATSAT forecast errors themselves. Fig. 34 shows the evolution of the forecast errors in time.

6. CONCLUSIONS

The OSEs described here demonstrate that the AFGL GDAS is operating satisfactorily. In particular the agreement between the STATSAT and NMC analyzed 500 mb height fields is typically 40 (50) m in the Northern (Southern) Hemisphere (Fig. 11). This is smaller than the usual 60 or 80 m contour interval usually used to draw 500 mb charts. In addition, subjective comparison of the 500 mb analyses revealed no unusual differences. At 1000 mb there are however substantial differences due, no doubt, to different usage of the surface observations. We should compare initialized analyses to determine if these differences are important from the point of view of the forecast. Differences in the Southern Hemisphere are more substantial. In the Southern Hemisphere there are much fewer radiosondes and the analyses must rely much more on available satellite data and the model forecasts. There are notable differences between the NMC and ASAP procedures for using the satellite height information which might account for the differences in the Southern Hemisphere. In particular, ASAP analyzes height while McPherson et al. (1979) analyze temperature. Also, in the February case, we used larger observational error variances for the satellite heights (cf. Table 1, p. 6).

The NOSAT, NOCON and NOCOR experiments delineate the impact of satellite data on the AFGL GDAS. Since only conventional data are used in NOSAT, the differences between NOSAT and STATSAT analyses are mainly found over the oceans. However, the first guess advects errors from the data-sparse to data-rich regions. Thus there are substantial differences throughout the Southern Hemisphere and smaller differences along the western edges of the Northern Hemisphere land masses. Forecast differences are small (large) in the Northern (Southern) Hemisphere. We note that when there is not much data available (as in the NOSAT experiment) the resulting forecasts may be poor yet agree very well with the analyses.

A novel aspect of our conventional data denial experiments is that we

have denied all Type 1, 2 and 3 data in the NOCON and NOCOR experiments. In other conventional data denial experiments reported in the literature surface observations (Type 3) are usually retained in the data mix. In the present experiments no use is made of surface observations to anchor the satellite thicknesses. Without conventional data in the Northern Hemisphere, the quality of the analyses decays over the 7 day assimilations. Beyond 7 days this quality would probably continue to decay to the level of current operational Southern Hemisphere analyses. Such a data system is clearly inferior to the STATSAT (full FGGE) system. However, for the first few days of data denial such a system may be adequate. It is clear from the NOCOR experiment that the GDAS is successful at propagating information from the data rich to the data denied region. However, it is also clear that in the winter errors propagate across the Pacific extremely quickly. This highlights the global nature of numerical weather prediction.

Although we have tried to make a fairly complete assessment of these 4 experiments, some questions are still open, and further work will be undertaken to answer them. It is not clear, for example, whether comparing the different forecasts to the NMC analysis allows an unbiased evaluation. This will be checked by computing the RMS differences between forecasts and radiosonde data. Anomaly correlations will also be computed. Other points to be investigated are the effect of the normal mode initialization on the analyzed fields, especially its effect on the noisiness of the fields, and the impact of the use of satellite data on the wind fields.

The experiments reported here serve to define the baseline for future experiments planned and underway with the AFGL GDAS and to provide calibration with impact studies conducted by other investigators. Certainly the AFGL system will be the subject of future refinements and evolution. In the near term and of particular interest are the following enhancements and planned experiments: Better physical parameterizations for the GSM will be used in future data assimilation experiments. We will under this contract evaluate the impact of these parameterizations on the GDAS. We will attempt to make better use of available moisture information in another impact test. We will use either a level by level approach following Norquist (1986) to relate auxillary information to humidity, or we will relate 3DNEPH cloud information to moisture profiles using statistical methods which we are currently

investigating. The impact of improved temperature and moisture retrievals prepared by Susskind et al. (1984) and by AER will be determined in two further data impact experiments. The experiment using the Susskind data is now under way. In addition minor improvements to the ASAP procedures are being developed and will be tested by repeating a portion of one of the experiments. We also are using the AFGL GDAS in a series of OSSEs now underway.

7. References

Atlas, R., M. Ghil, and M. Halem, 1982a: The effect of model resolution and satellite sounding data on GLAS model forecasts. Mon. Weather Rev., 110, 662-682.

Ballish, B., 1980: Initialization, theory and application to the NMC spectral model. Ph.D. Thesis, Dept. of Meteorology, University of Maryland, College Park, MD, 151 pp.

Bergman, K. H., 1979: Multivariate analysis of temperature and winds using optimum interpolation. Mon. Weather. Rev., 107, 1423-1444.

Brenner, S., C-H. Yang, and S. Y. K. Yee, 1982: The AFGL spectral model of the moist global atmosphere: Documentation of the baseline version. AFGL-TR-82-0393, AFGL, Hanscom AFB, MA, 65 pp. [NTIS ADA129283].

Brenner, S., C.-H. Yang, and K. Mitchell, 1984: The AFGL global spectral model: Expanded resolution baseline version. AFGL-TR-84-0308, AFGL, Hanscom AFB, MA 72 pp. [NTIS ADA160370].

Dey, C. H., and L. L. Morone, 1985: Evolution of the National Meteorlogical Center Global Data Assimilation System: January 1982-December 1983. Mon. Weather Rev., 113, 304-318.

Gilchrist, A., 1982: JSC study conference on observing systems experiments. Exeter, 19-22 April 1982. GARP/WCRP Numerical Experimentation Program, Rep. 4, 83 pp.

Gutowski, W. J., and R. N. Hoffman, 1985: Robust data quality control in a statistical interpolation scheme. In Preprints, Ninth Conference on Probability and Statistics in Atmospheric Sciences, October 9-11, 1985, Virginia Beach, VA, American Meteorological Society, Boston, MA, pp. 428-433.

Halberstam, I., C. Johnson, D. C. Norquist, and S.-L. Tung, 1984: Two methods of global data assimilation. AFGL-TR-84-0260, AFGL, Hanscom AFB, MA., 91 pp. [NTIS ADA155981].

Isaacs, R. G., R. N. Hoffman, and L. D. Kaplan, 1986: Remote sensing of geophysical parameters for numerical weather prediction. Rev. of Geophys., 24, 701-743.

Mather, P. M., 1976: Computational Methods of Multivariate Analysis in Phisical Geography. John Wiley, 532 pp.

McPherson, R. D., K. H. Bergman, R. E. Kistler, G. E. Rasch, and D. S. Gordon, 1979: The NMC operational global data assimilation system. Mon. Weather Rev., 107, 1445-1461.

McPherson, R. D., 1984: Cloud-drift wind estimates during FGGE. NMC Office Note 288, US DOC/NOAA/NWS/NMC, 13 pp.

Norquist, D. C., 1982a: Adaptation and application of NMC nonlinear normal mode initialization scheme. In Objective Analysis and Prediction Techniques, A. M. Gerlach (ed.), AFGL-TR-82-0394, AFGL, Hanscom AFB, MA, pp. 21-32 [NTIS ADA131465].

Norquist, D. C., 1982b: Development of objective analysis schemes using the method of optimum interpolation. In Objective Analysis and Prediction Techniques, A. M. Gerlach (ed.), AFGL-TR-82-0394, AFGL, Hanscom AFB, MA, pp. 51-55 [NTIS ADA131465].

Norquist, D. C., 1983: Development and testing of a multivariate global statistical analysis system. In Objective Analysis and Prediction Techniques, A. M. Gerlach (ed.), AFGL-TR-83-0333, AFGL, Hanscom AFB, MA, pp. 10-48 [NTIS ADA142441].

Norquist, D. C., 1984: Users guide for optimum interpolation method of global data assimilation. AFGL-TR-84-0290, AFGL, Hanscom AFB, MA., 67 pp. [NTIS ADA155929].

Norquist, D. C., 1986b: Alternative forms of moisture information in 4-D data assimilation. AFGL-TR-86-0194, AFGL, Hanscom AFB, MA, 71 pp. [NTIS ADA179792].

Phillips, N. A., 1976: The impact of synoptic observing and analysis systems on flow pattern forecasts. Bull. Am. Meteorol. Soc., 57, 1225-1240.

Sela, J. G., 1980: Spectral modeling at the National Meteorological Center. Mon. Weather Rev., 108, 1279-1292.

Susskind, J., J. Rosenfield, D. Reuter, and M. T. Chahine, 1984: Remote sensing of weather and climate parameters from HIRS/MSU on TIROS-N. J. Geophys. Res., 89(D3), 4677-4697.

Tung, S. L., 1983: Generalization and application of Machenhauer initialization scheme. In Objective Analysis and Prediction Techniques, A. M. Gerlach (ed.), AFGL-TR-83-0333, AFGL, Hanscom AFB, MA, [NTIS ADA142441].

Appendix A

Super-Observations (super-obs)

We have developed a procedure to form super-obs from the FGGE Level II cloud drift winds (CDWs). While doing this we discovered that the final reprocessed data set contains many duplicate observations. Each pair of duplicate observations contains an original observation and a quality controlled observation; the only difference between the two are the quality control flags.

The purpose of super-obbing is to compress large data sets containing highly correlated and hence redundant observations. Employing redundant data can make the mathematics of the OI problem ill-conditioned, and it also reduces the efficiency of the procedure. In addition, the AFGL OI may ignore large blocks of data because of core space limitations; compressing redundant data should reduce, if not eliminate, this problem. CDWs in particular are often very closely spaced (hence redundant) and very numerous (frequently > 5,000 in a 6-hour period).

Some forecast centers employ rigorous data selection to thin large data sets, but this procedure does not necessarily eliminate redundance. We have followed a procedure similar to the European Centre for Medium Range Weather Forecasts (ECMWF) and formed super-obs by merging together highly correlated observations. We form super-obs in a preprocessing step before the data are made available to the OI.

After eliminating duplicate reports in favor of the more recent NASA/NMC special effort quality controlled data, the super-obbing program forms cluster of data points to be combined by following four steps:

1) Observations are assigned to latitude-longitude boxes. These are our initial clusters.
2) All nearby pairs of clusters are examined. Pairs which are close enough together are merged.
3) Each observation is examined to see if it would be better assigned to a different cluster. "Better" here means that the total variance within clusters is reduced. (See Mather, 1976, Section 6.15.) Steps 2 and 3 are repeated until there are no changes.

4) Observations and/or super-observations within the cluster are then combined pairwise. At each stage the closest pair is combined into a super-ob. When the separation between the closest pair exceeds the critical distance (equal to 200 km) the procedure for this cluster stops.

When two observations, either of which may be a super-obs already, are combined into a super-obs, all associated fields are combined. In this way the output data set is similar in form and content to the input data set. One additional field, the number of observations combined, must be included. For measured quantities, we form a weighted average. For variability estimates, we form a weighted average of variances. The weights are the number of (super-)observations in each of the two inputs. For quality control flags, the minimum quality is assigned to the new super-obs. Type indices are retained if both inputs agree; otherwise they are set to unknown. For the FGGE Level II CDWs the specific actions taken are listed in table A.1. For quality control flags two matrices ITAB30 and ITAB36 are used. ITAB30 and ITAB36 are based on Tables XXX and XXXVI of Appendix A of FGGE Formats. For ITAB30, if *i-1 and j-1 are the values for Table XXX for the two observations, then* ITAB30(i,j) is the corresponding value assigned to the combined observation. ITAB30 is filled so that it returns the lower quality value of i-1 and j-1. The "not specified" category overrides all others but "low level..." ITAB36 is based on the same general principals as ITAB30. "No quality control" overrides all others except "probably incorrect," "incorrect" and "erroneous." Otherwise, the lower quality value of the pair is returned. Code 4 is not defined (and should never be referenced); it is arbitrarily reassigned to code 3 ("erroneous") using the table.

Note that:

(1) Observations separated by more than 100 mb are not combined.

(2) Observations with IQCP or IQC not equal to 0, 1, 5, 6, 7 (i.e., unacceptable observations) are not used.

(3) Distance used by the program is chord (or Cartesian) distance, not great circle distance.

Table A.1

Pairwise combination procedure for observation characteristics.

(The symbolic names are taken from Norquist, 1984)

Item	Name	Procedure
1	ALAT	Weighted average
2	ALONG	Weighted average, accounting for Greenwich.
3	IDA	Keep if they agree; otherwise account for midnight
4	IHR	Weighted average, accounting for midnight
5	IDSI	Keep. Will always agree.
6	ITSWD	Keep if inputs agree; zero otherwise
7	PRES	Weighted average
8	IQCP	Assign with ITAB30
9	IQC	Assign with ITAB36
10	TEMP	Weighted average
11	WD	Weighted average, accounting for due North
12	WS	Weighted average
13	IQCWD	Assign with ITAB30
14	IQCWS	Assign with ITAB30
15	OEVE	Rms weighted average
16	OEPE	Rms weighted average
17	IEHM	Set to zero if either is zero; otherwise weighted average
18	PDC	Weighted average
19	ICC	Keep if inputs agree; zero if either is zero; 9 otherwise
20	ISWFP	Keep if inputs agree; zero otherwise
21	NOBS	Add

We changed the OI so that it recognizes the new quality flags. We did not alter the observational errors of the super-obbed CDW because the errors of the original data are so highly correlated.

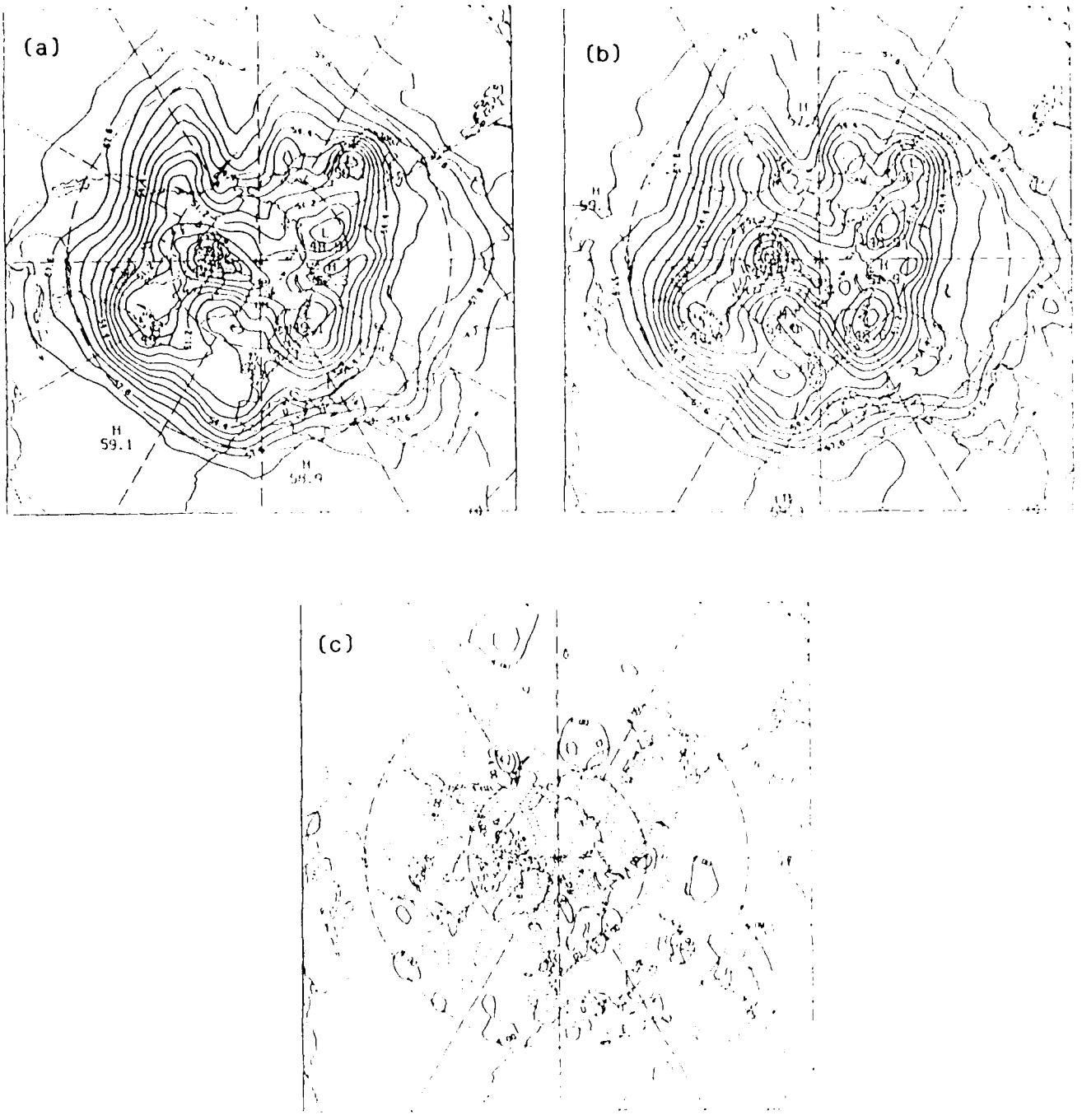

Fig. 1. The STATSAT (a) and NMC (b) 500 mb height analyses for the Northern Hemisphere at 00 GMT 11 February 1979 and their difference (STATSAT minus NMC (c). In (a) and (b) and in succeeding maps of 500 mb height the contour interval is 80 m. In (c) and in succeeding maps of 500 mb height difference (or error) the contour interval is 40 m and the zero line has been suppressed for clarity.

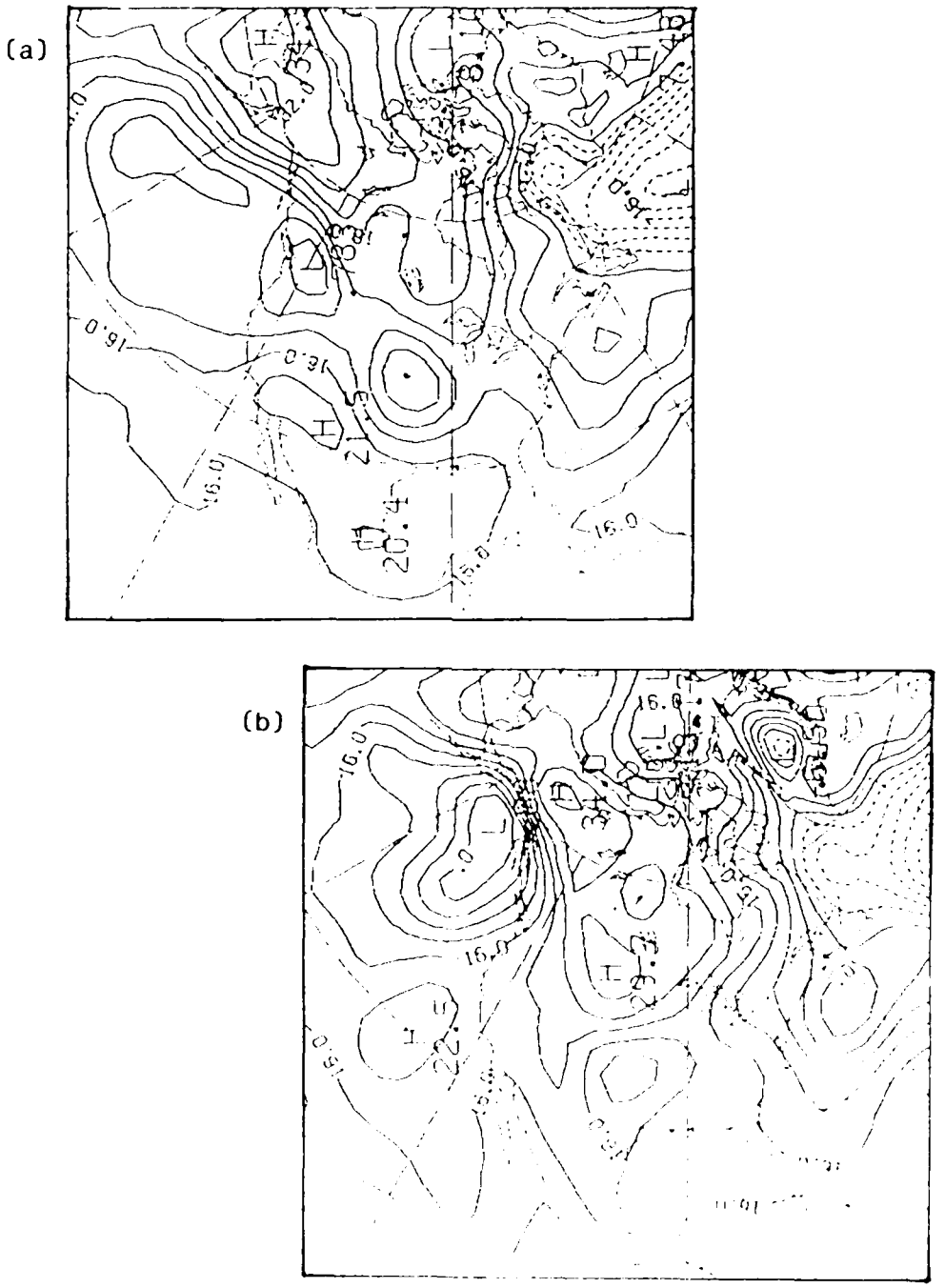

Fig. 2. The STATSAT (a) and NMC (b) 1000 mb height analyses for North America at 12 GMT 8 February 1979. Here and in succeeding maps of 1000 mb height the contour interval is 40 m

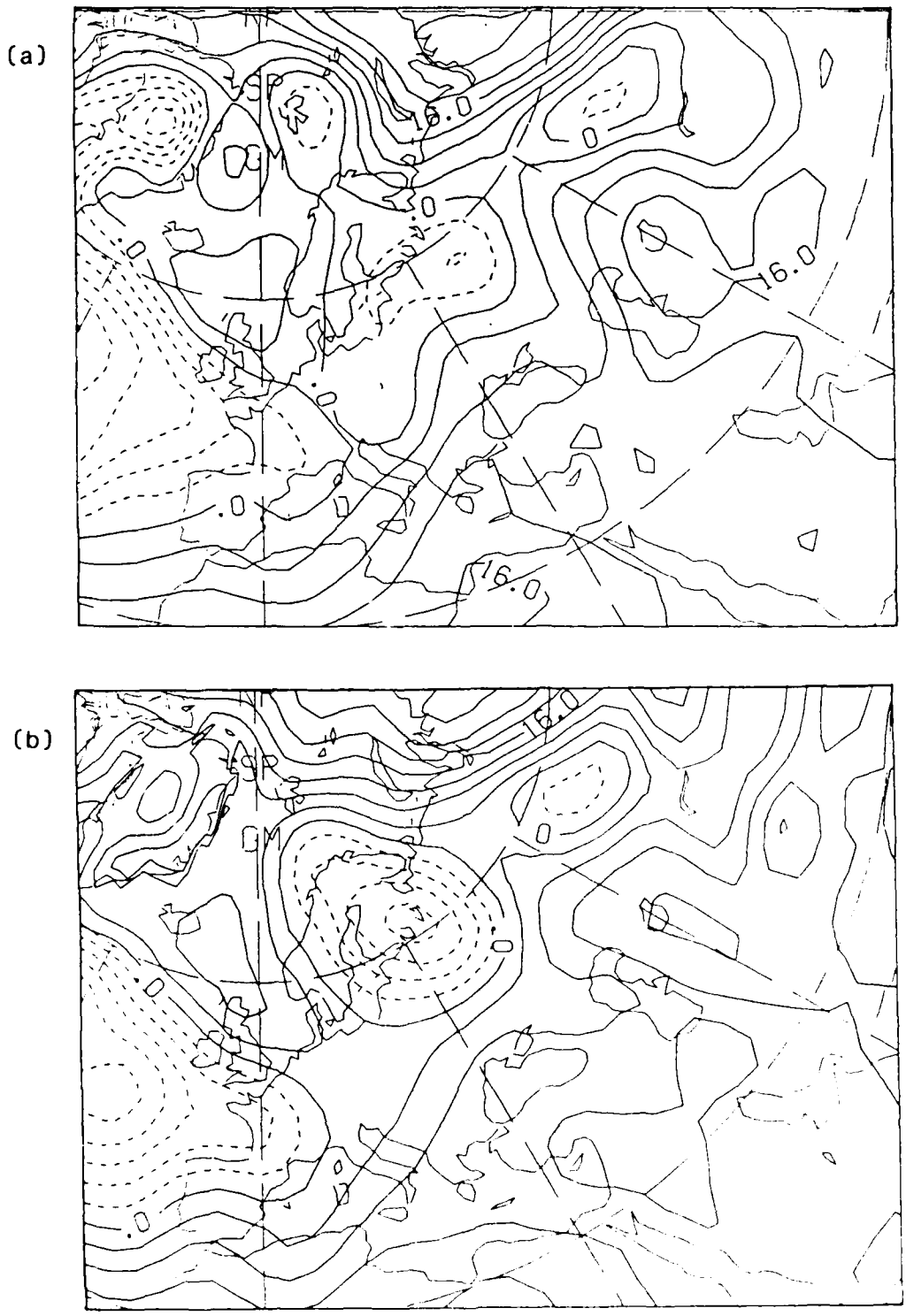

Fig. 3. The STATSAT (a) and NMC (b) 1000 mb height analyses for Europe at 00 GMT 10 February 1979.

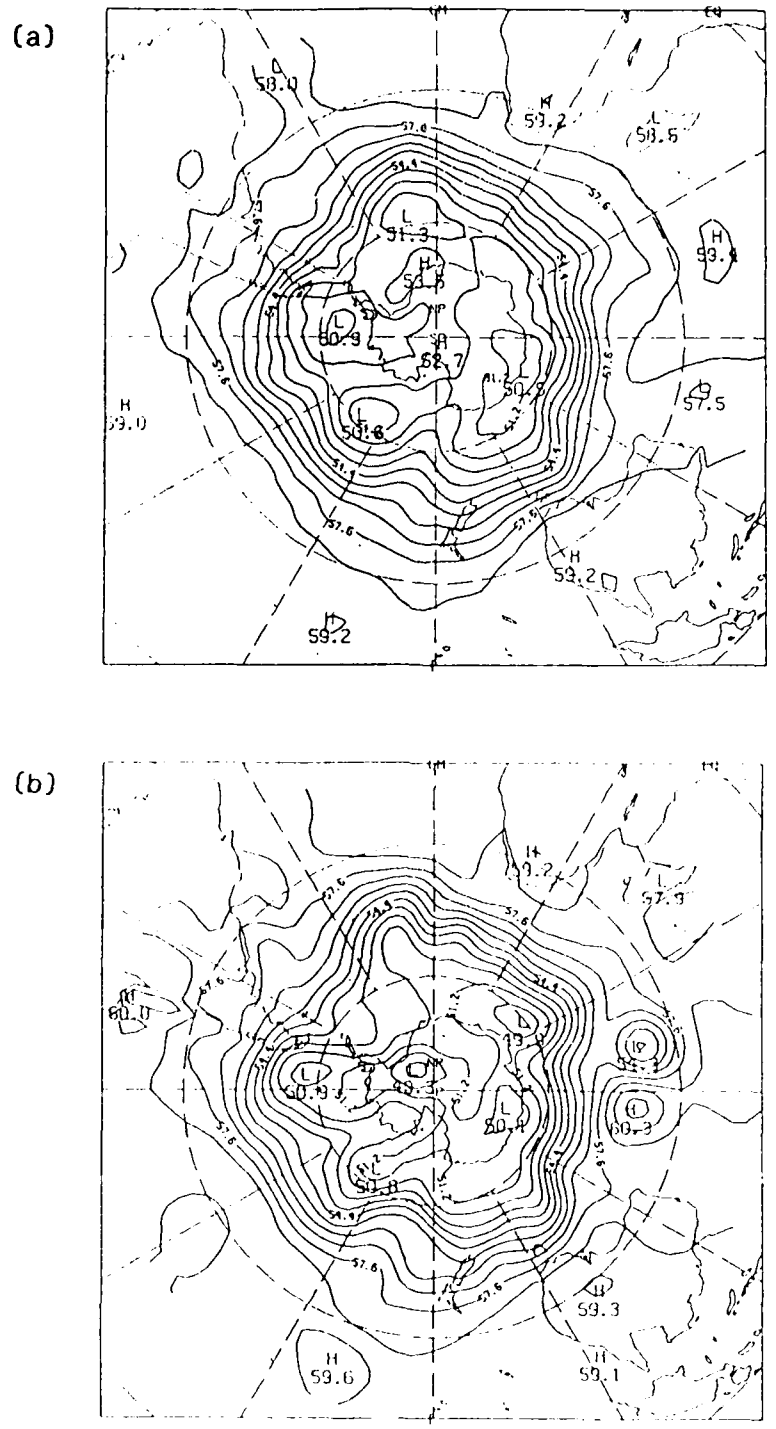

Fig. 4. The STATSAT (a) and NMC (b) 500 mb height analyses for the Southern Hemisphere at 00 GMT 13 February 1979.

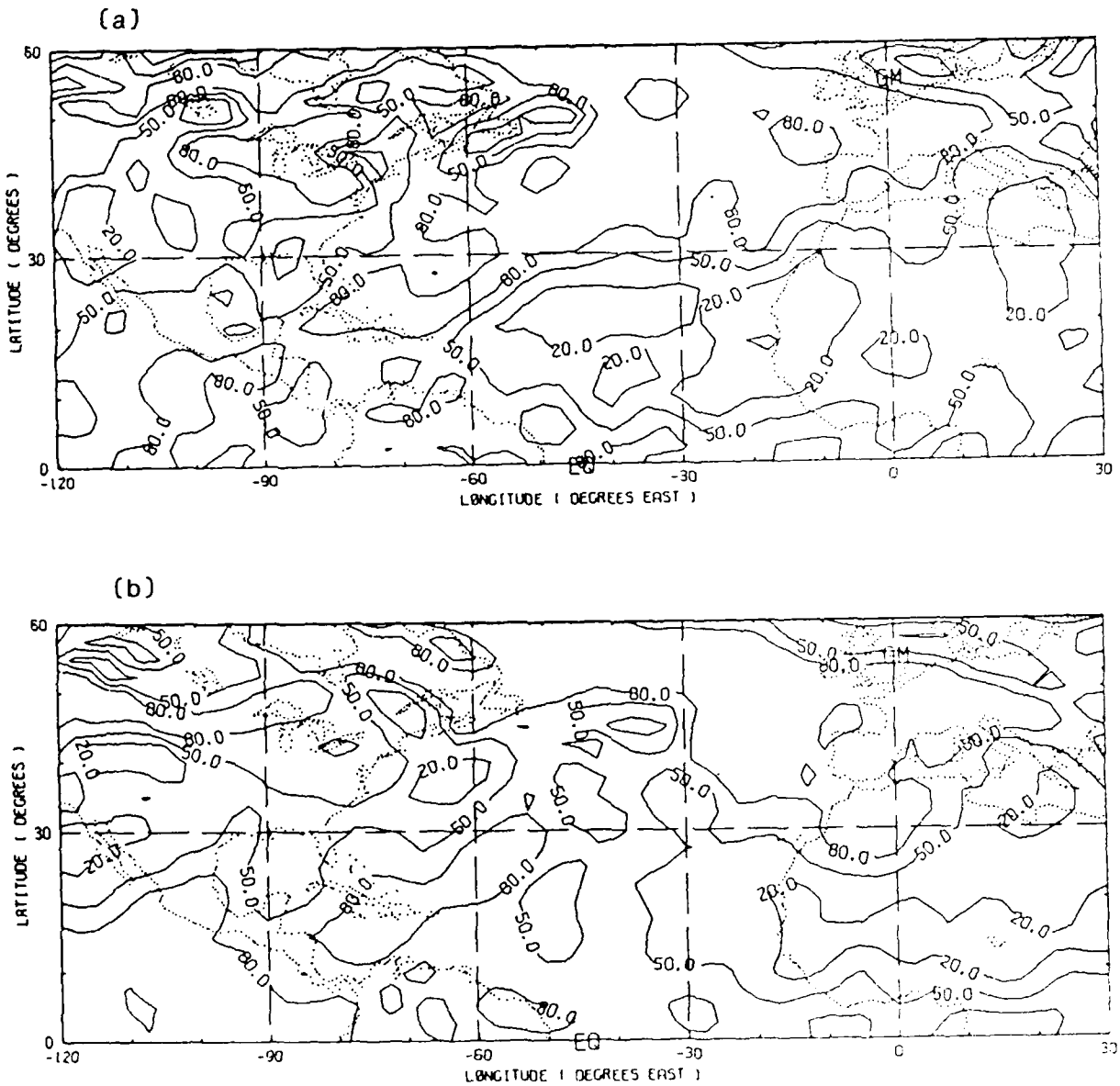

Fig. 5. The STATSAT (a) and NMC (b) 850 mb relative humidity analyses for the North Atlantic region at 00 GMT 12 February 1979. Here and in succeeding maps of 850 mb relative humidity, contours are drawn at 20, 50 and 80 percent.

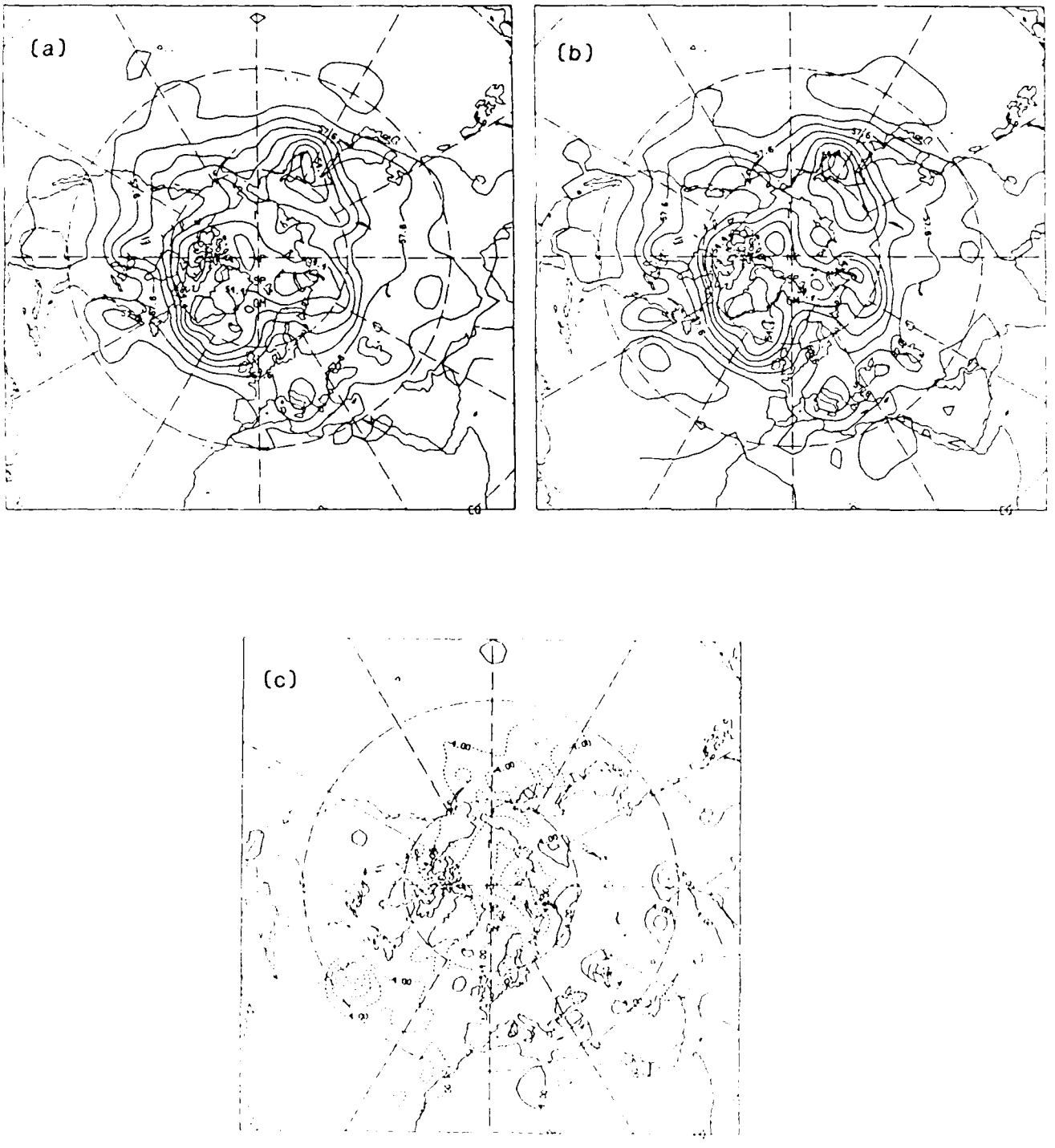

Fig. 6. The STATSAT (a) and NMC (b) 500 mb height analyses for the North Atlantic region at 00 GMT 21 June 1979 and their difference STATSAT NMC (c).

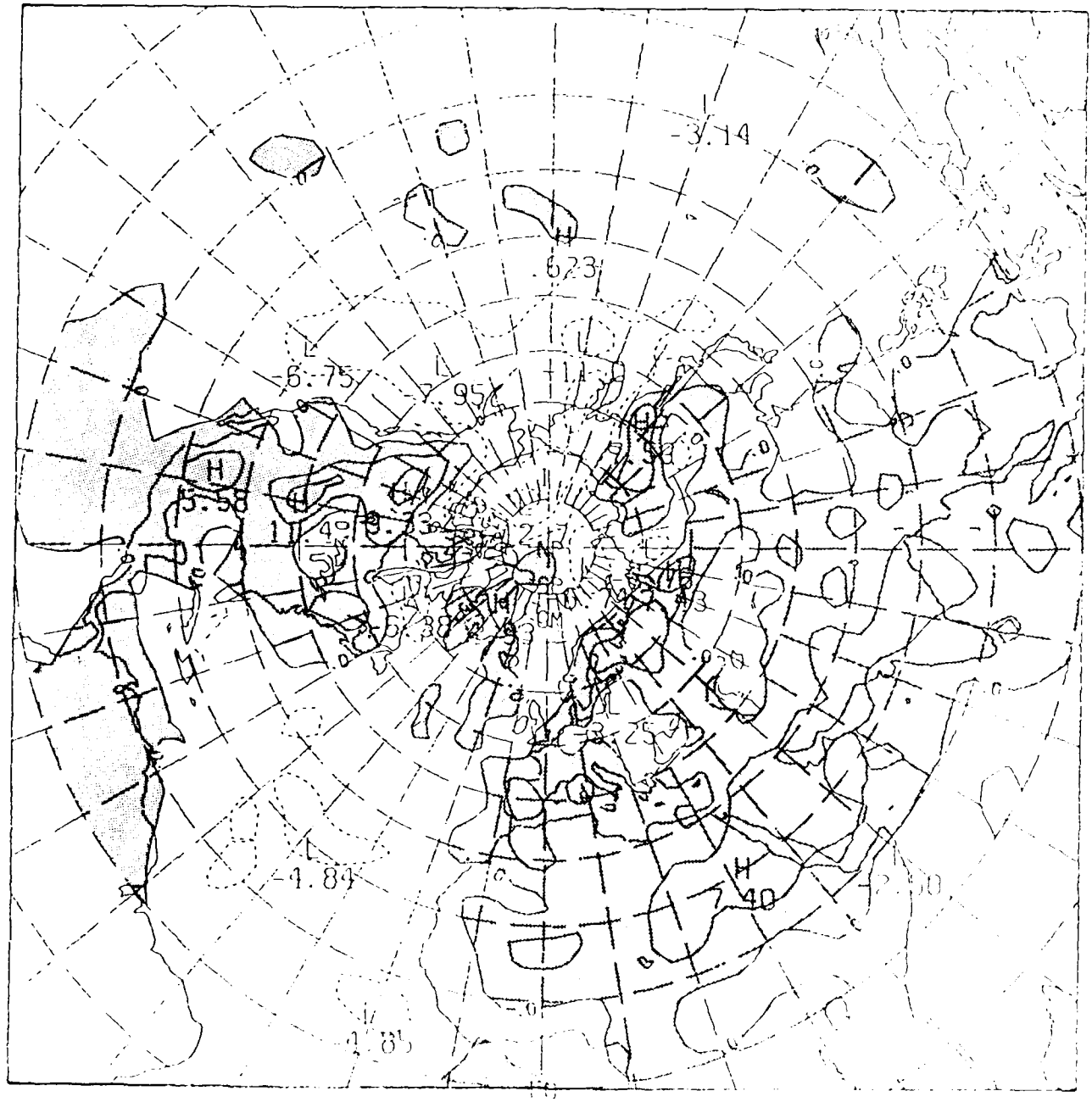

Fig. 7. The difference between STATSAT and NMC 1000 mb height analyses for the Northern Hemisphere at 00 GMT 18 June 1979. Here and in succeeding maps of 1000 mb height differences (or errors) the contour interval is 40 m. Positive differences are shaded.

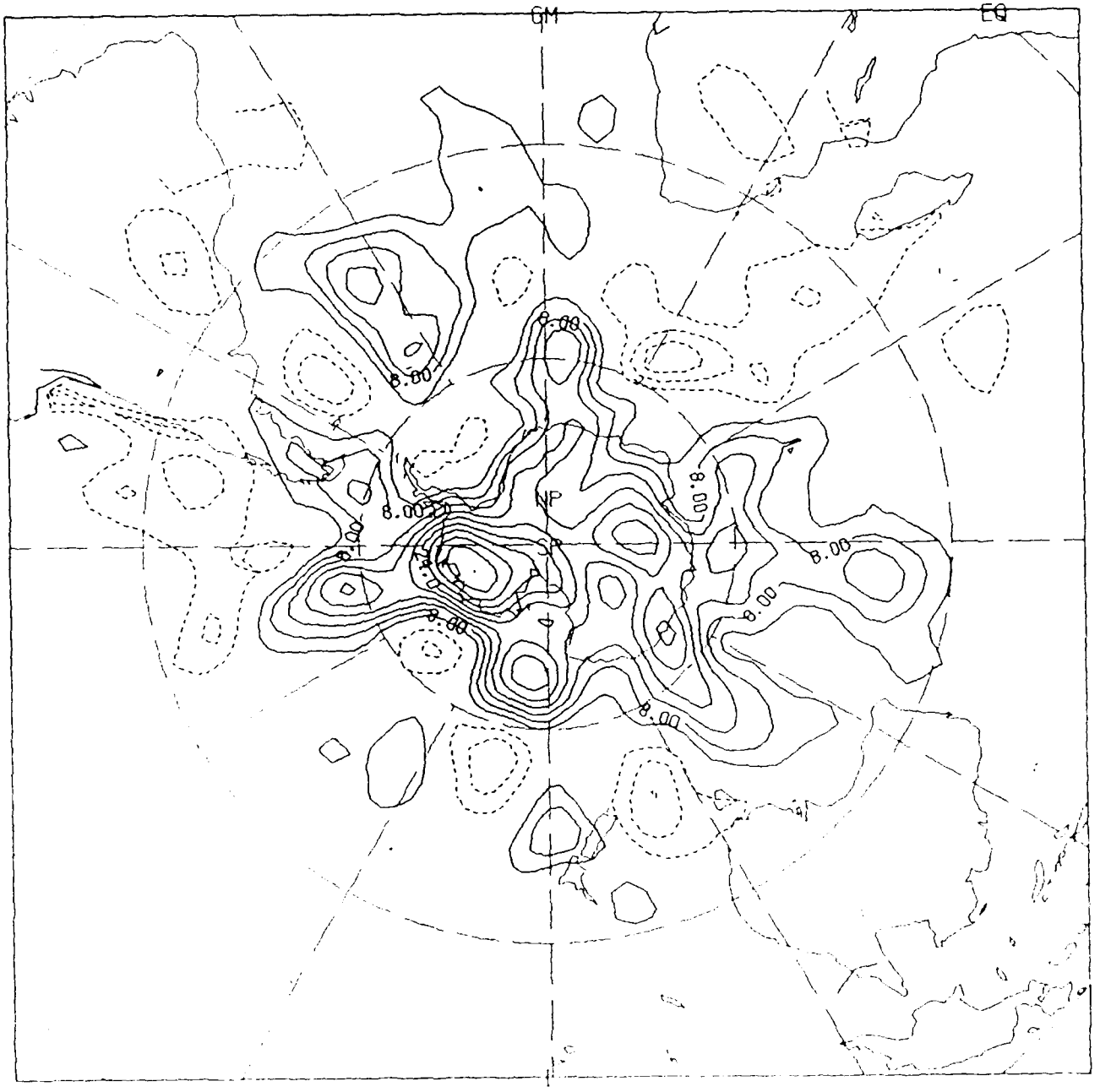

Fig. 8. The difference between STATSAT and NMC 500 mb height analyses for the Southern Hemisphere at 00 GMT 19 June 1979. In this and subsequent difference maps the zero line has been suppressed for clarity.

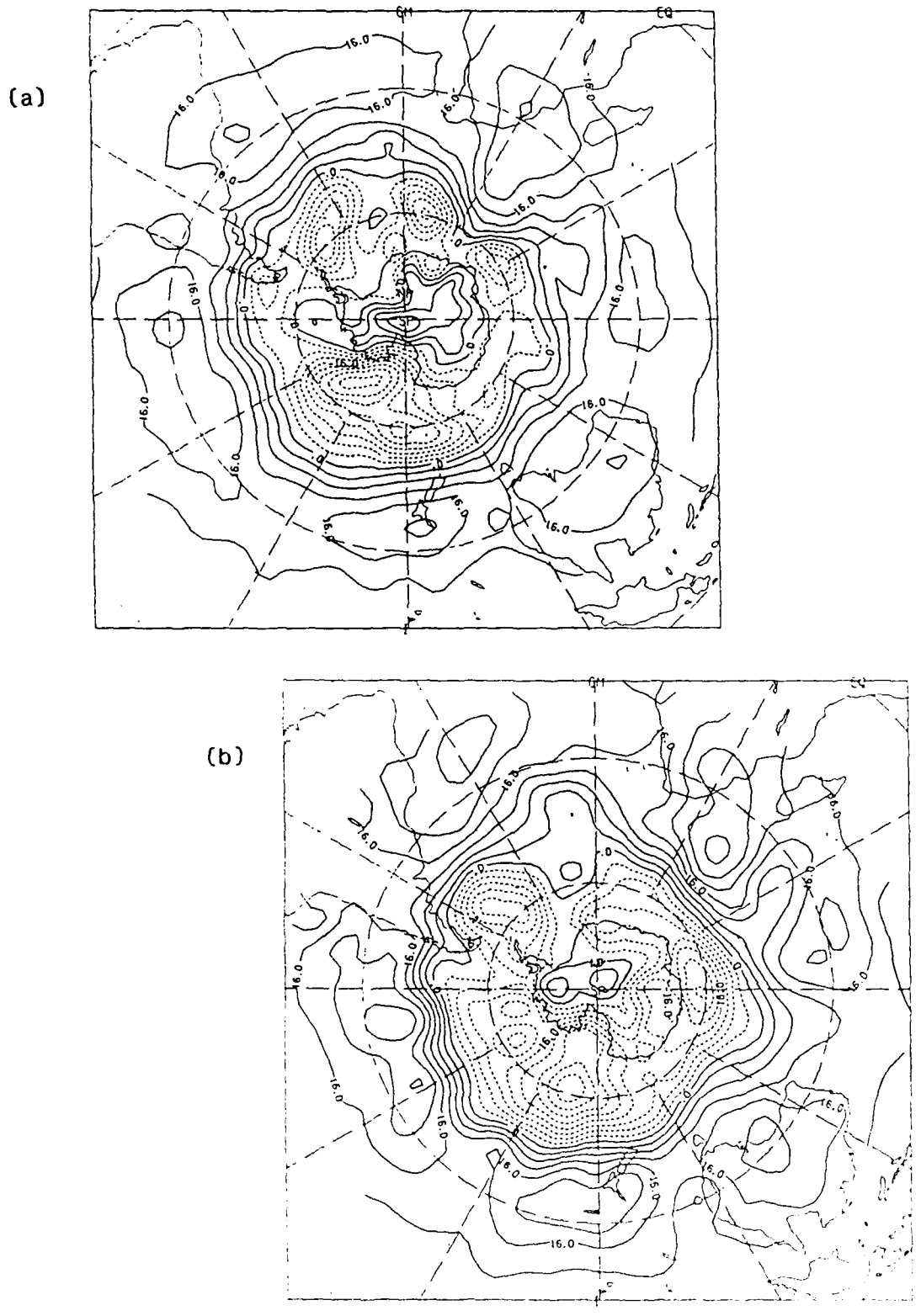

Fig. 9. The STATSAT (a) and NMC (b) 1000 mb height analyses for the Northern Hemisphere at 00 GMT 22 June 1979.

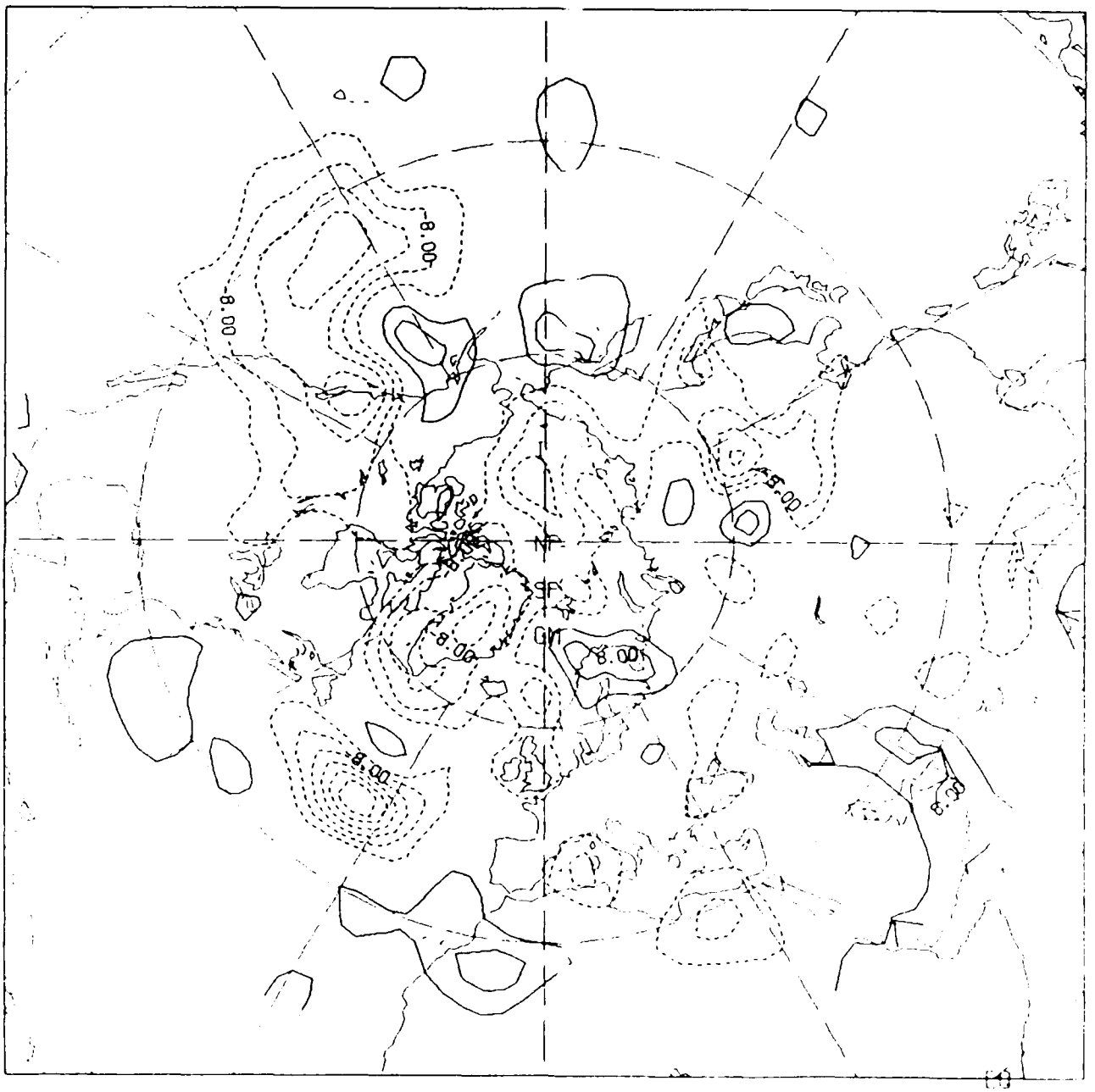

Fig. 10. The STATSAT - NMC 12 h 500 mb height forecast error for the Northern Hemisphere at 12 GMT 11 February 1979.

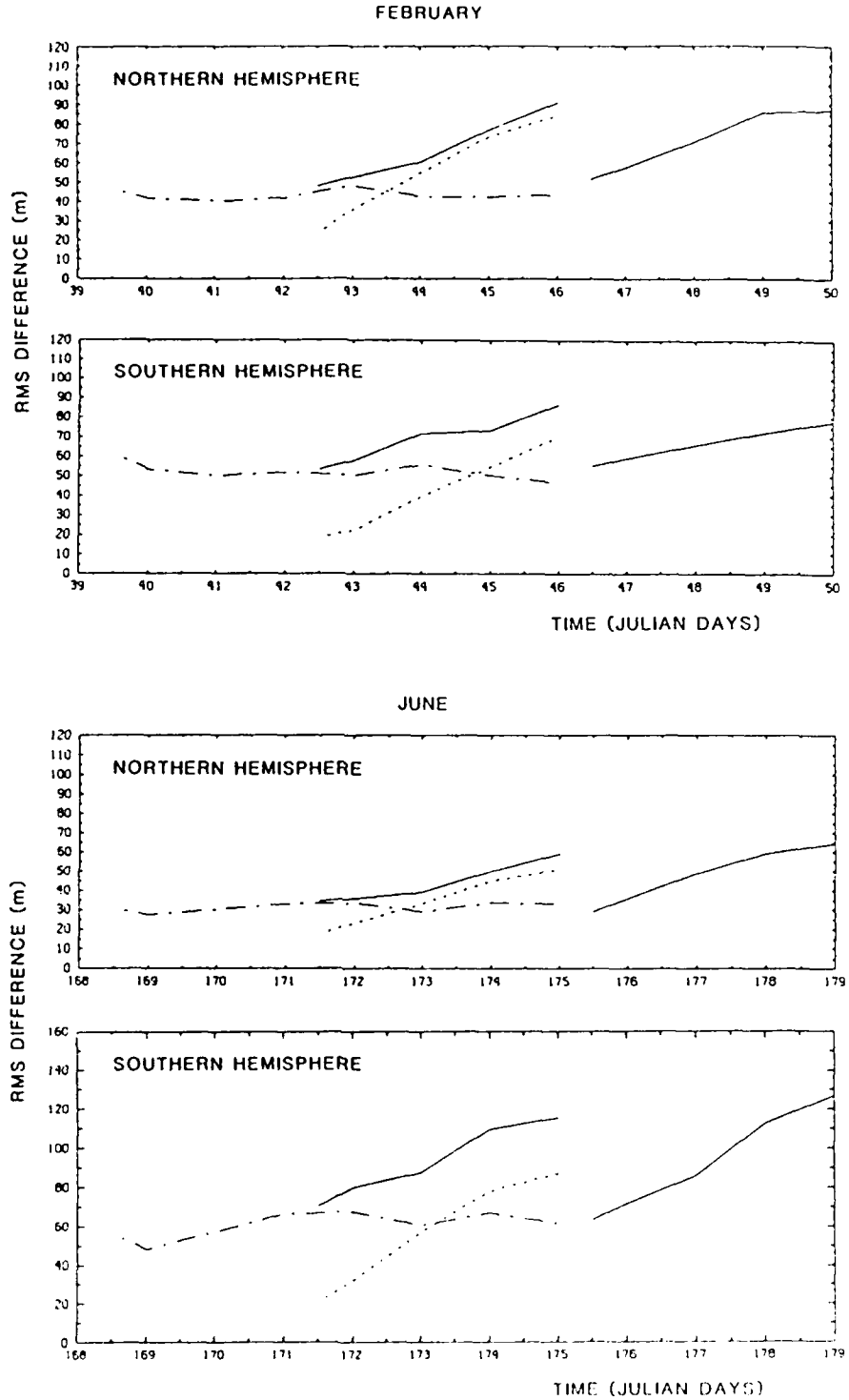

Fig. 11. Time evolution of rms differences between the 500 mb height analyses and forecasts. The comparisons shown are STATSAT analysis - NMC analysis (dot-dashed line), STATSAT forecast - NMC analysis (solid line) and STATSAT forecast - STATSAT analysis (dotted line). In this and succeeding figures of rms differences (or errors) each hemisphere and season is plotted separately.

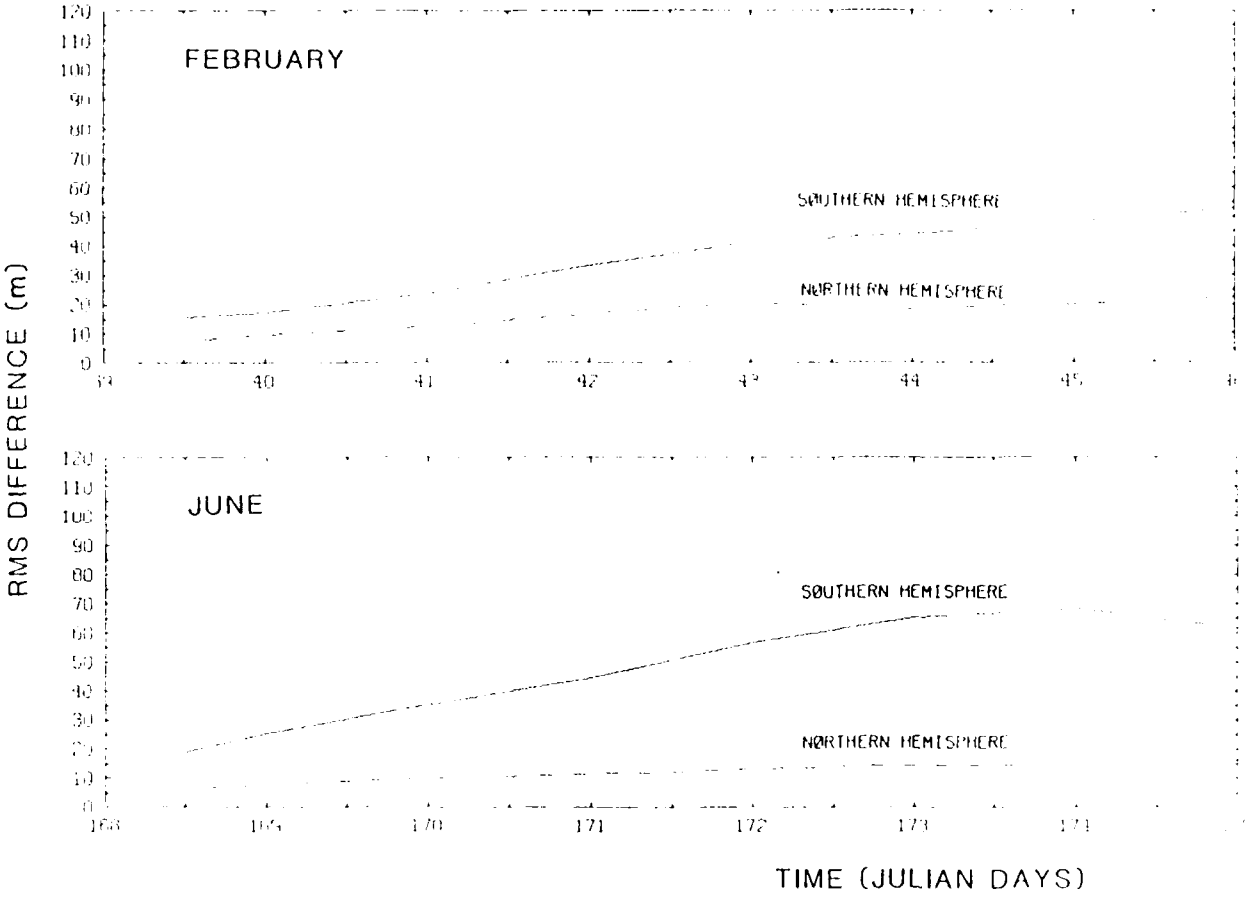

Fig. 12. Time evolution of rms differences between the NOSAT and [illegible] mb height analyses.

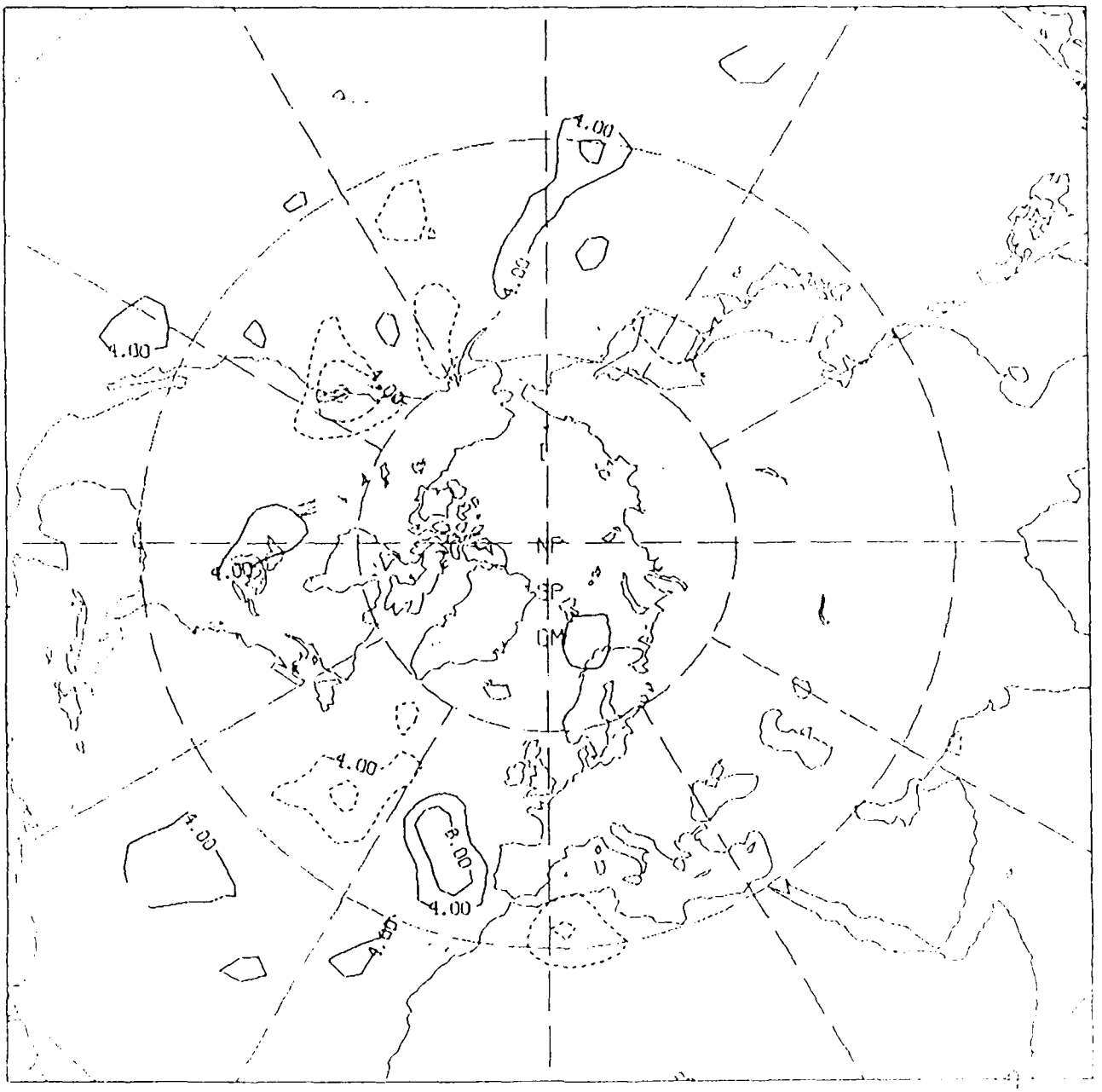

Fig. 13. The difference between NOSAT and STATSAT 500 mb height analyses for the Northern Hemisphere at 00 GMT 12 February 1979.

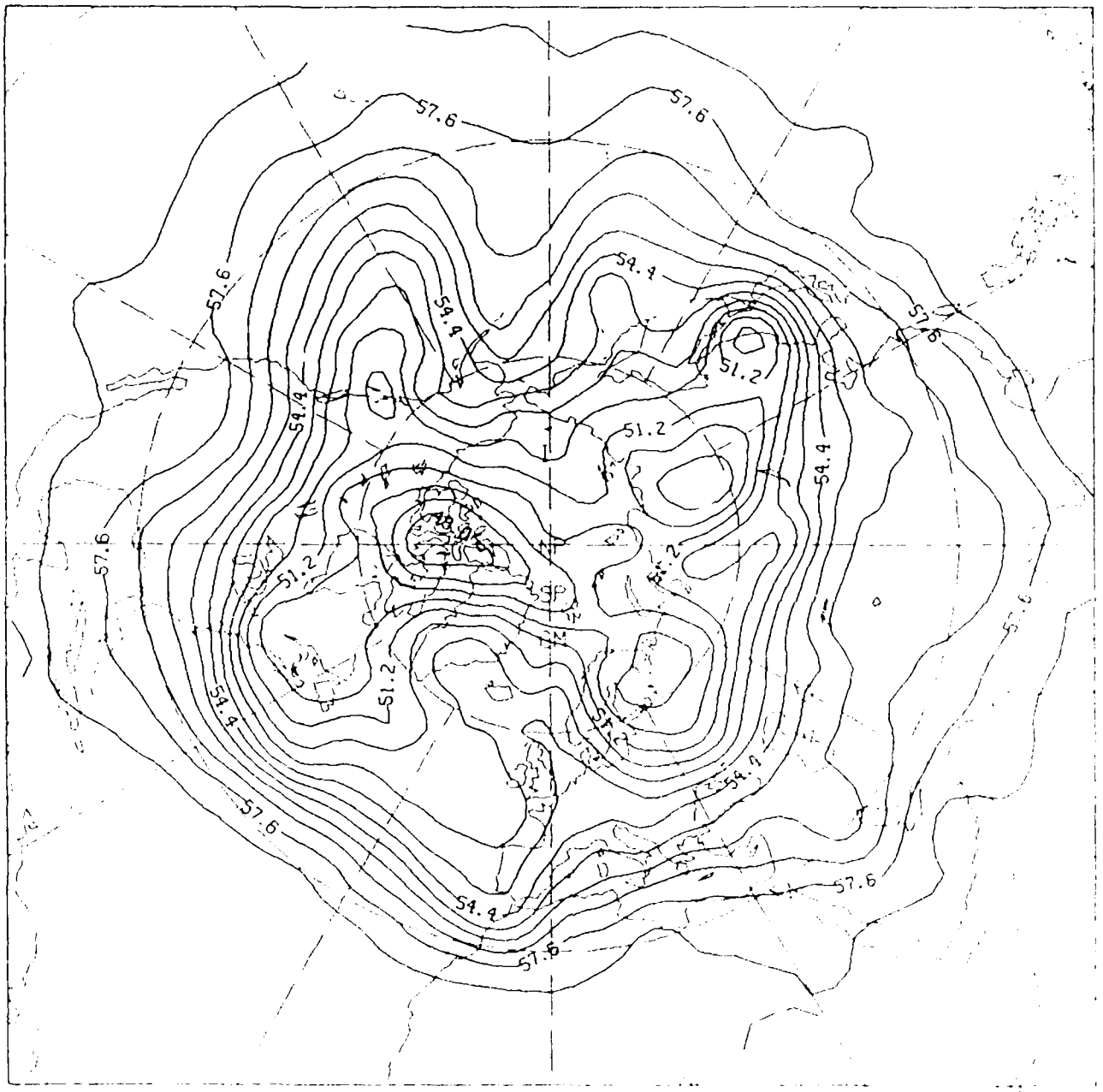

Fig. 14. The NOSAT 500 mb height analysis for the Northern Hemisphere at 00 GMT 11 February 1979. Compare with Fig. 1.

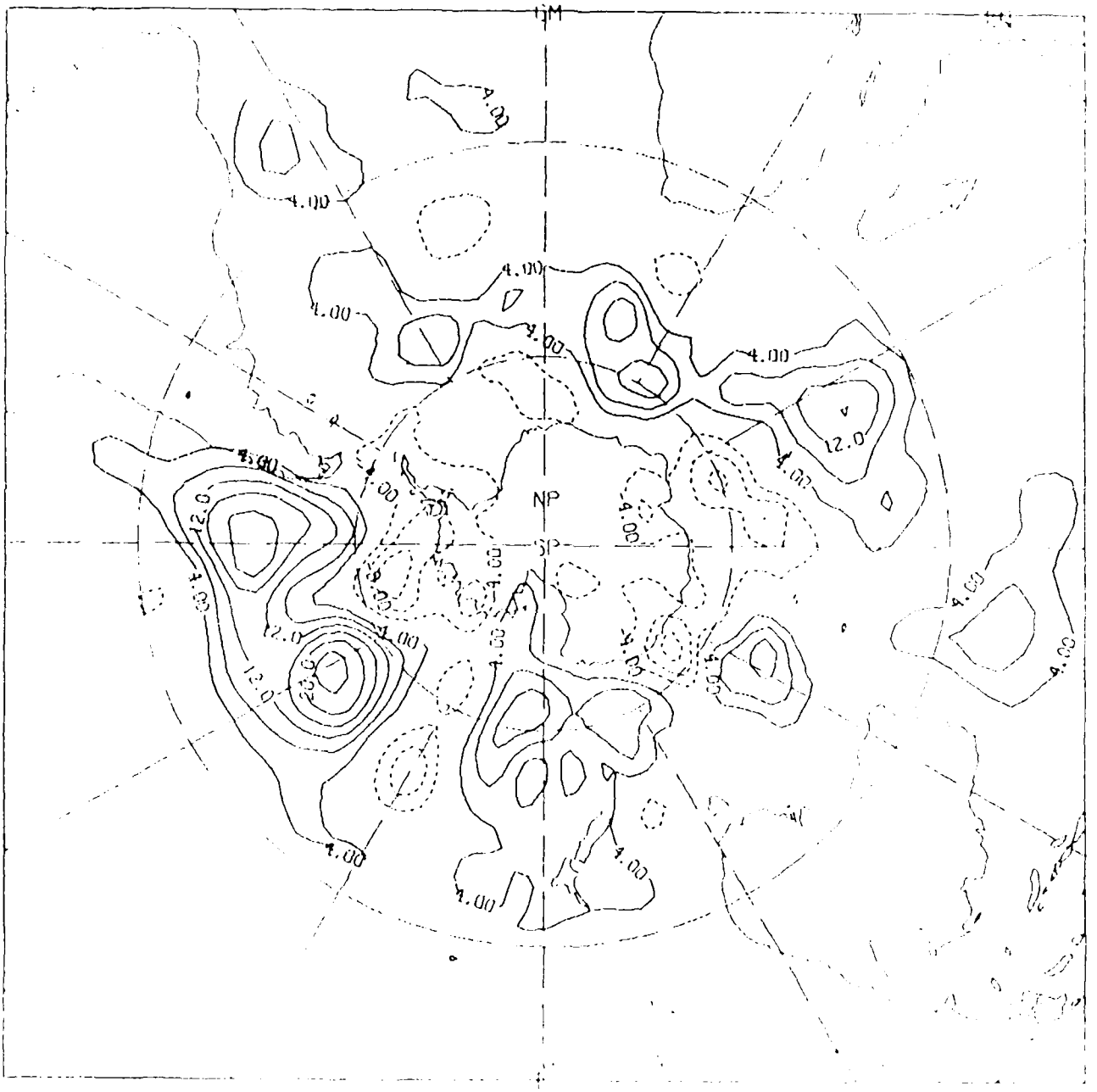

Fig. 15. The difference between NOSAT and STATSAT 500 mb height analyses for the Southern Hemisphere at 00 GMT 14 February 1979

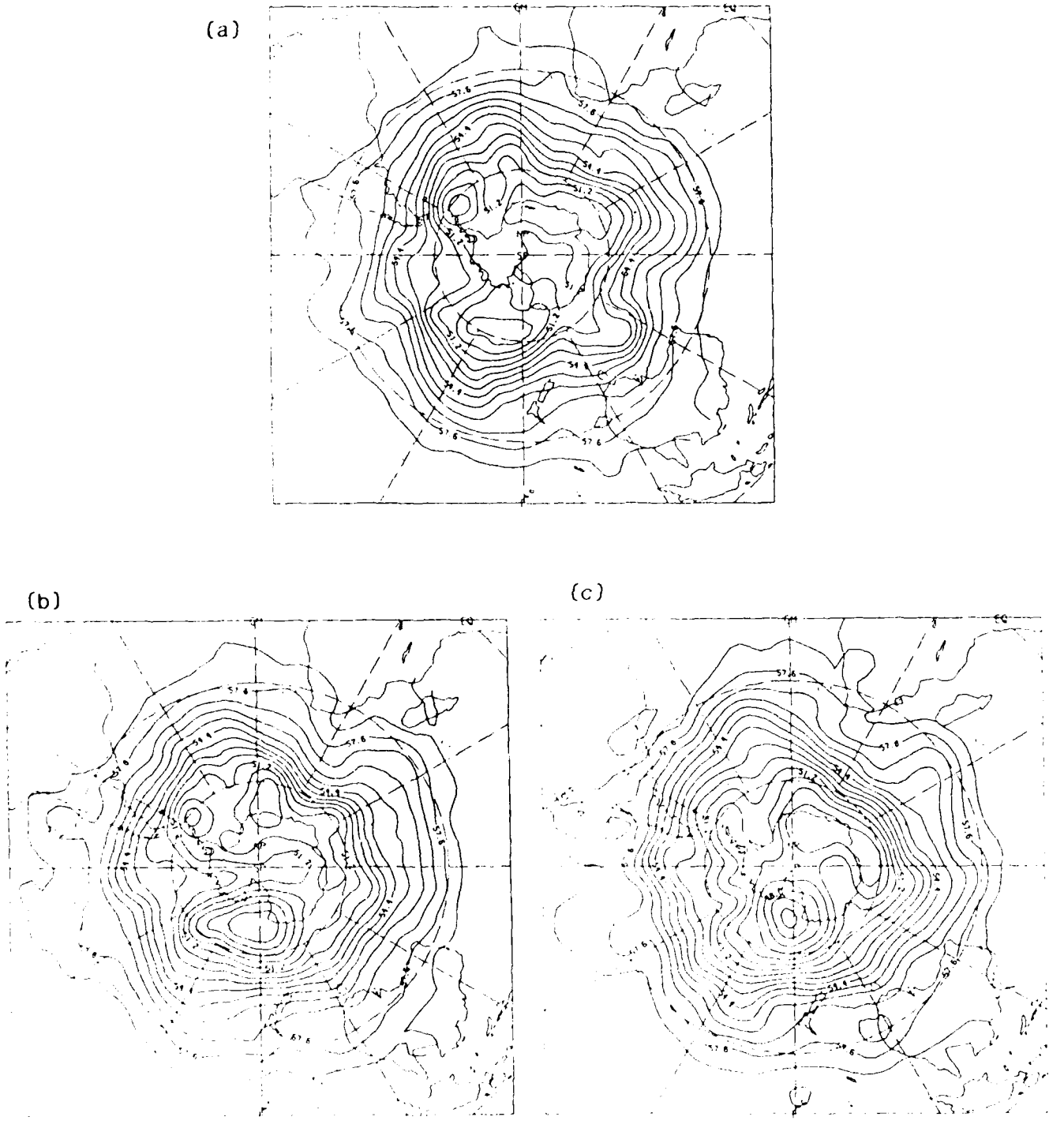

Fig. 16. The NOSAT (a), STATSAT (b) and NMC (c) 500 mb height analyses for the Southern Hemisphere at 00 GMT 22 June 1979.

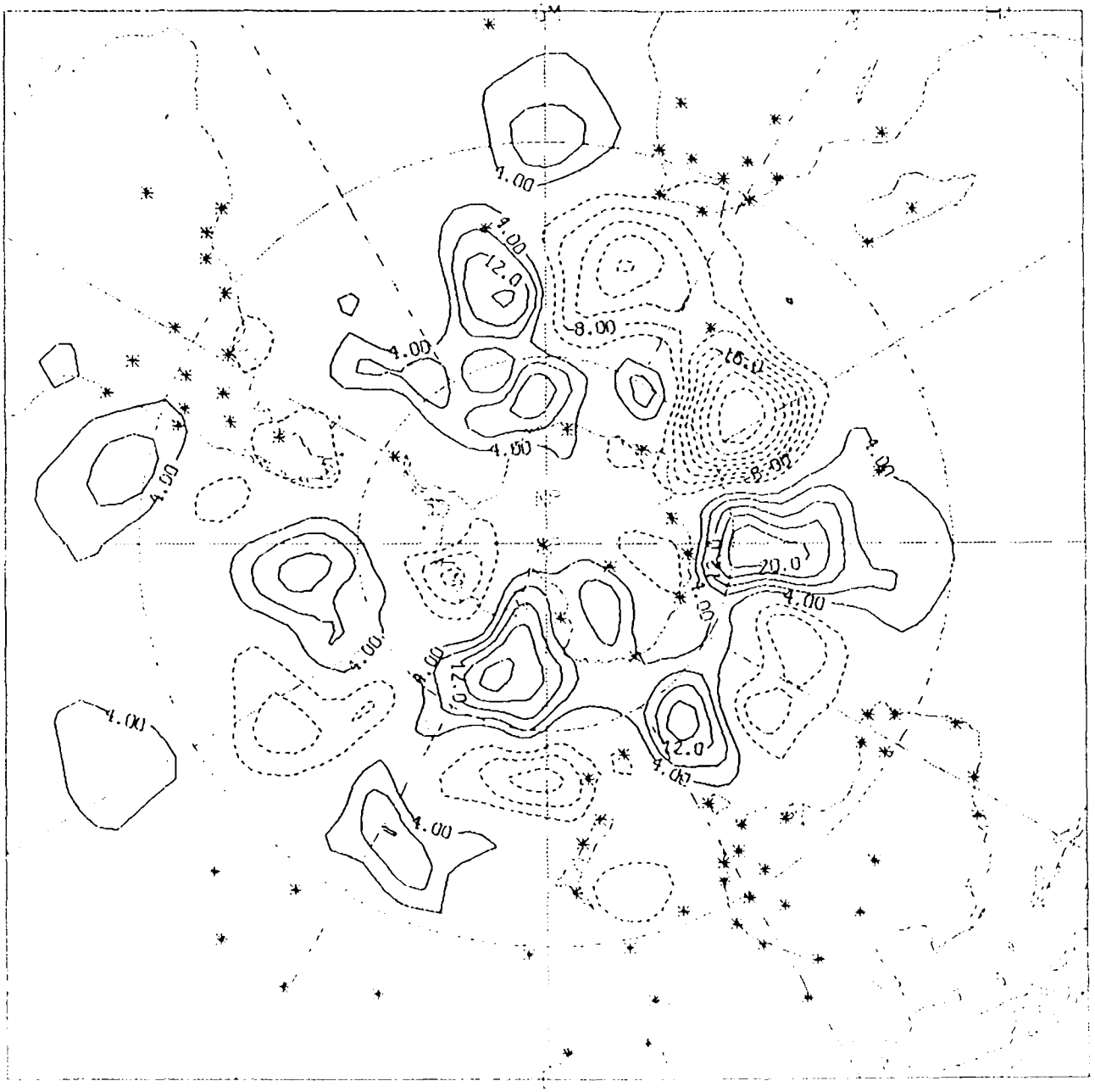

Fig. 17. The difference between NOSAT and STATSAT 500 mb height analyses for the Southern Hemisphere at 00 GMT 21 June 1979. The radiosonde stations are plotted as stars.

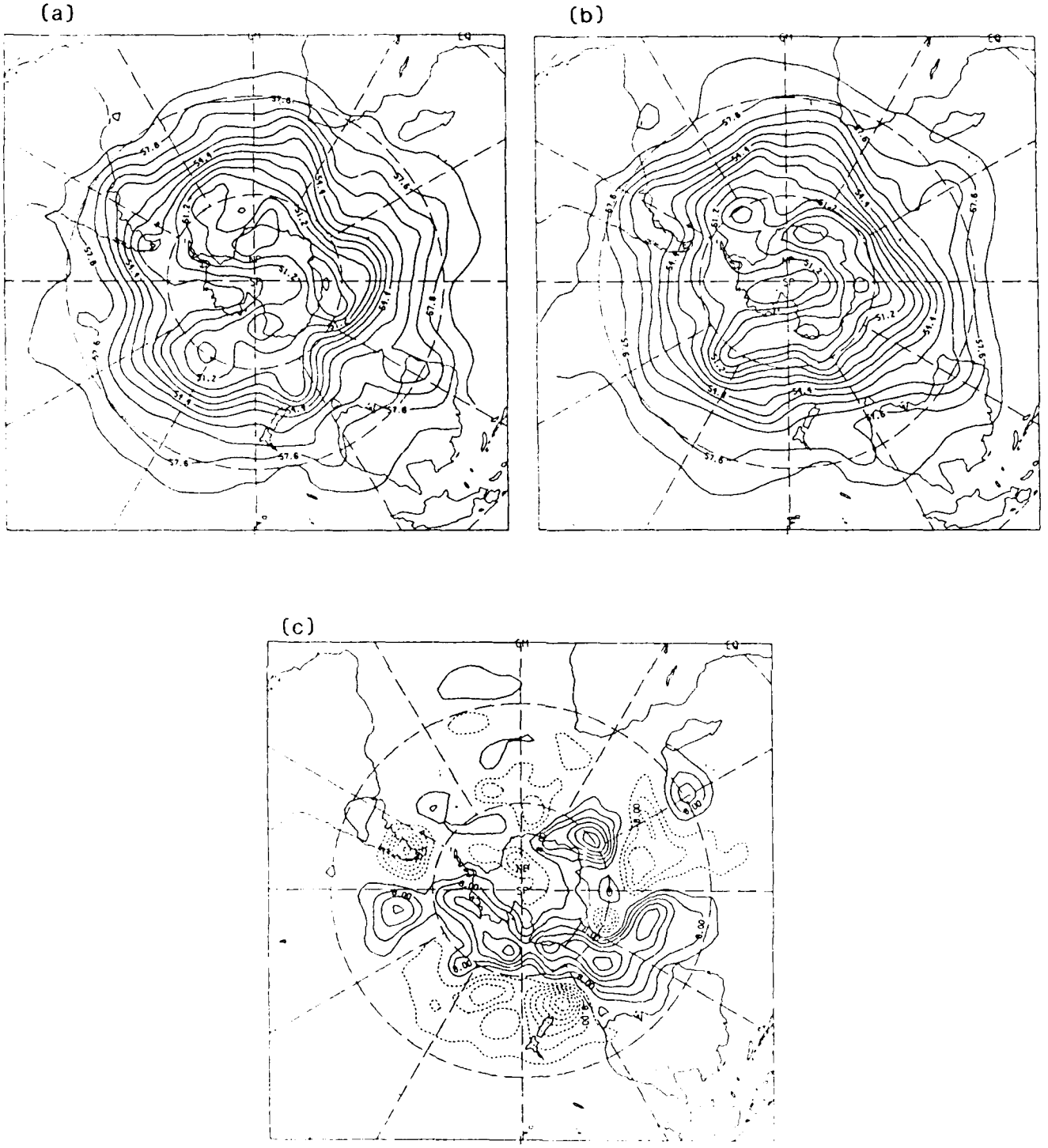

Fig. 18. The NOSAT (a) and STATSAT (b) 500 mb height analyses for the Southern Hemisphere at 00 GMT 24 June 1979 and their difference NOSAT - STATSAT.

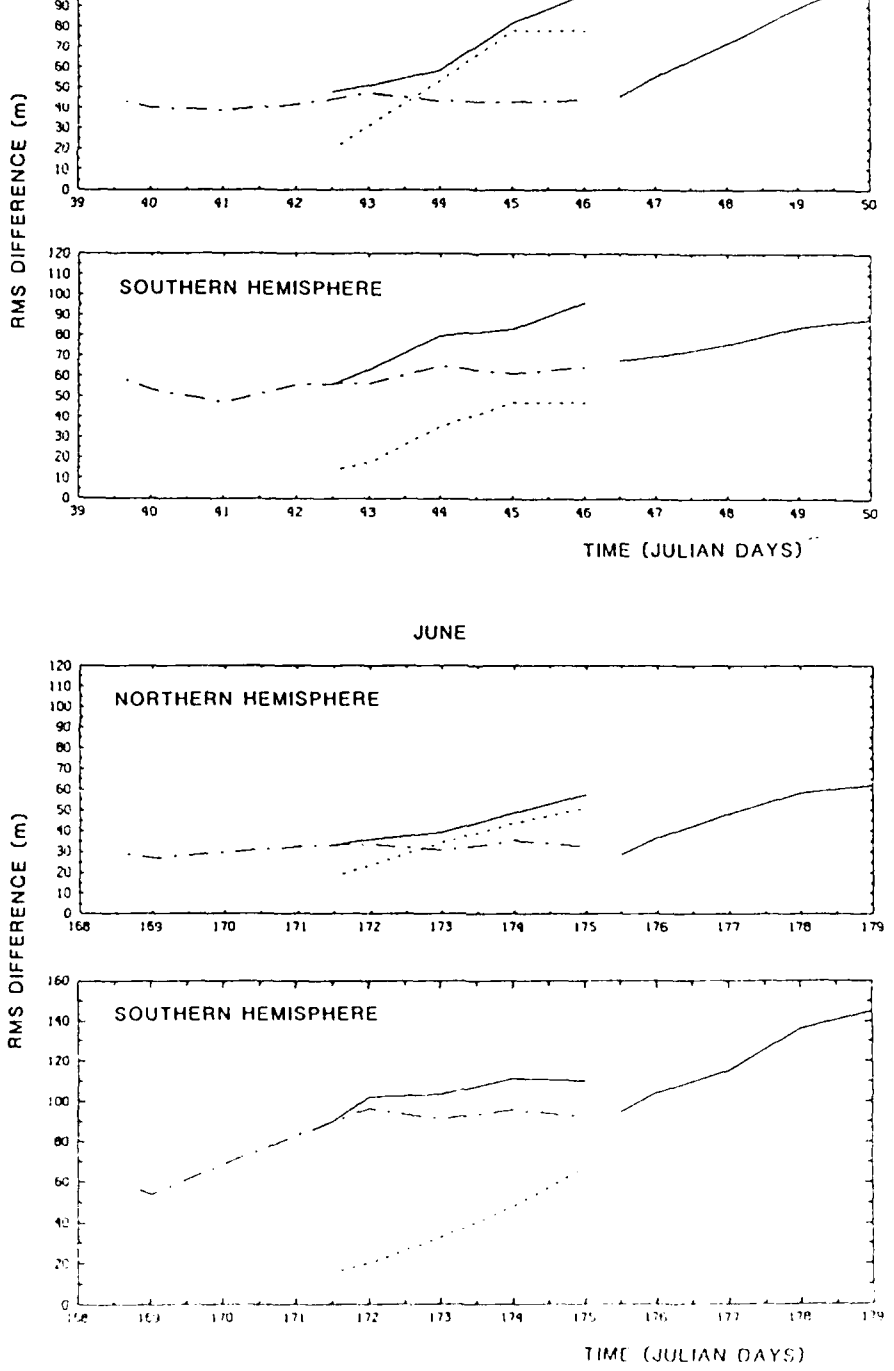

Fig. 19. Time evolution of rms differences between the 500 mb height analyses and forecasts. The comparisons shown are NOSAT analysis - NMC analysis (dot-dashed line), NOSAT forecast - NMC analysis (solid line) and NOSAT forecast - NOSAT analysis (dotted line).

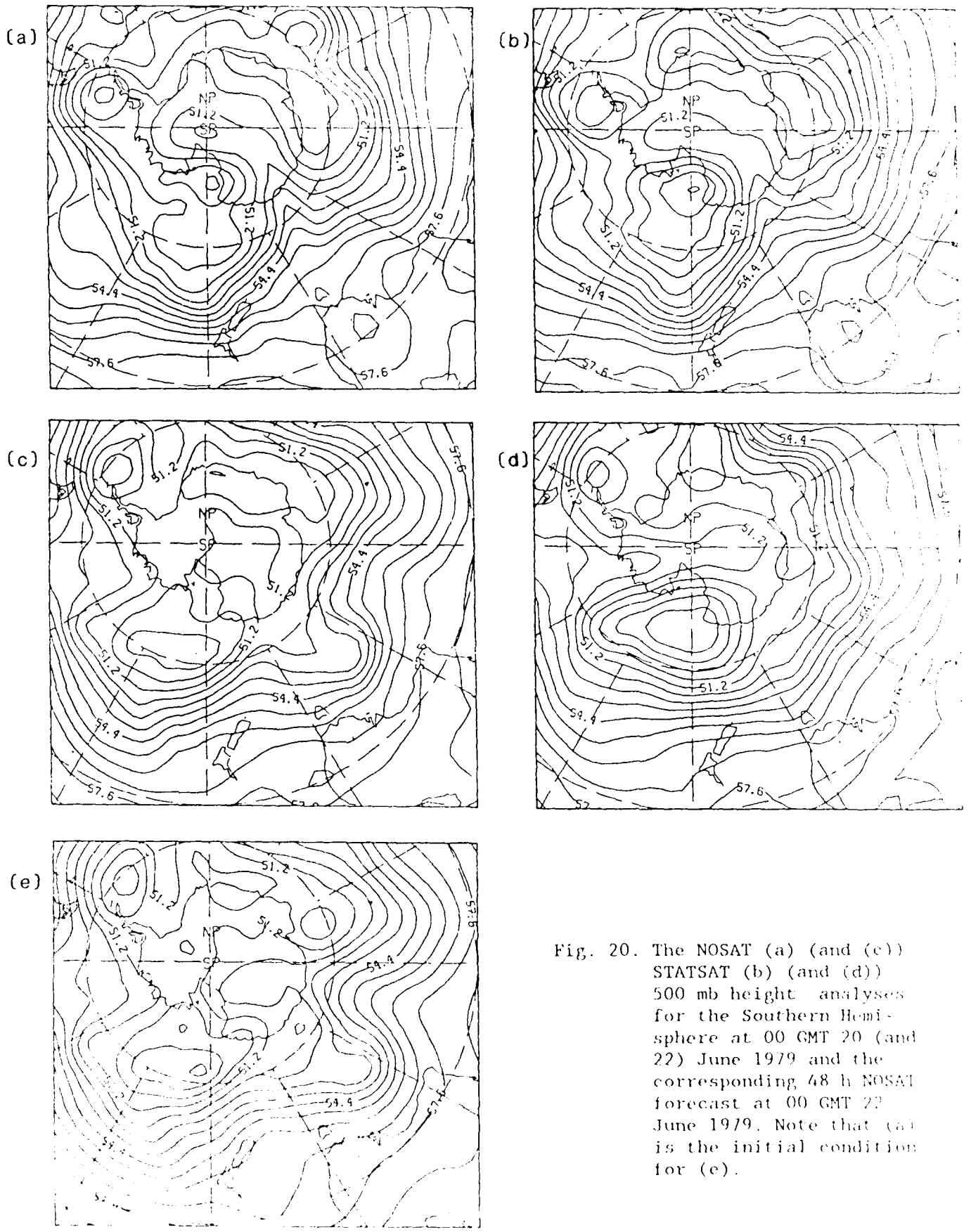

Fig. 20. The NOSAT (a) (and (c)) STATSAT (b) (and (d)) 500 mb height analyses for the Southern Hemisphere at 00 GMT 20 (and 22) June 1979 and the corresponding 48 h NOSAT forecast at 00 GMT 22 June 1979. Note that (a) is the initial condition for (e).

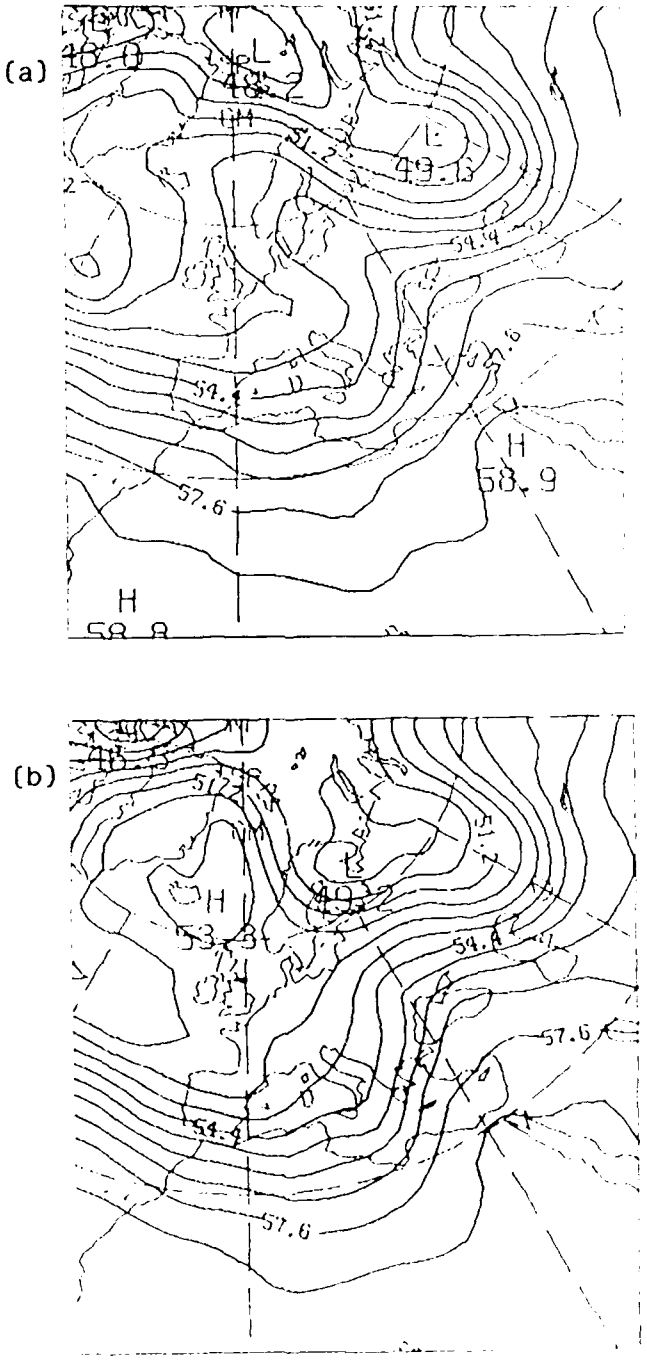

Fig. 21. The NOCON (a) and STATSAT (b) 500 mb height analyses for Europe at 00 GMT 13 February 1979.

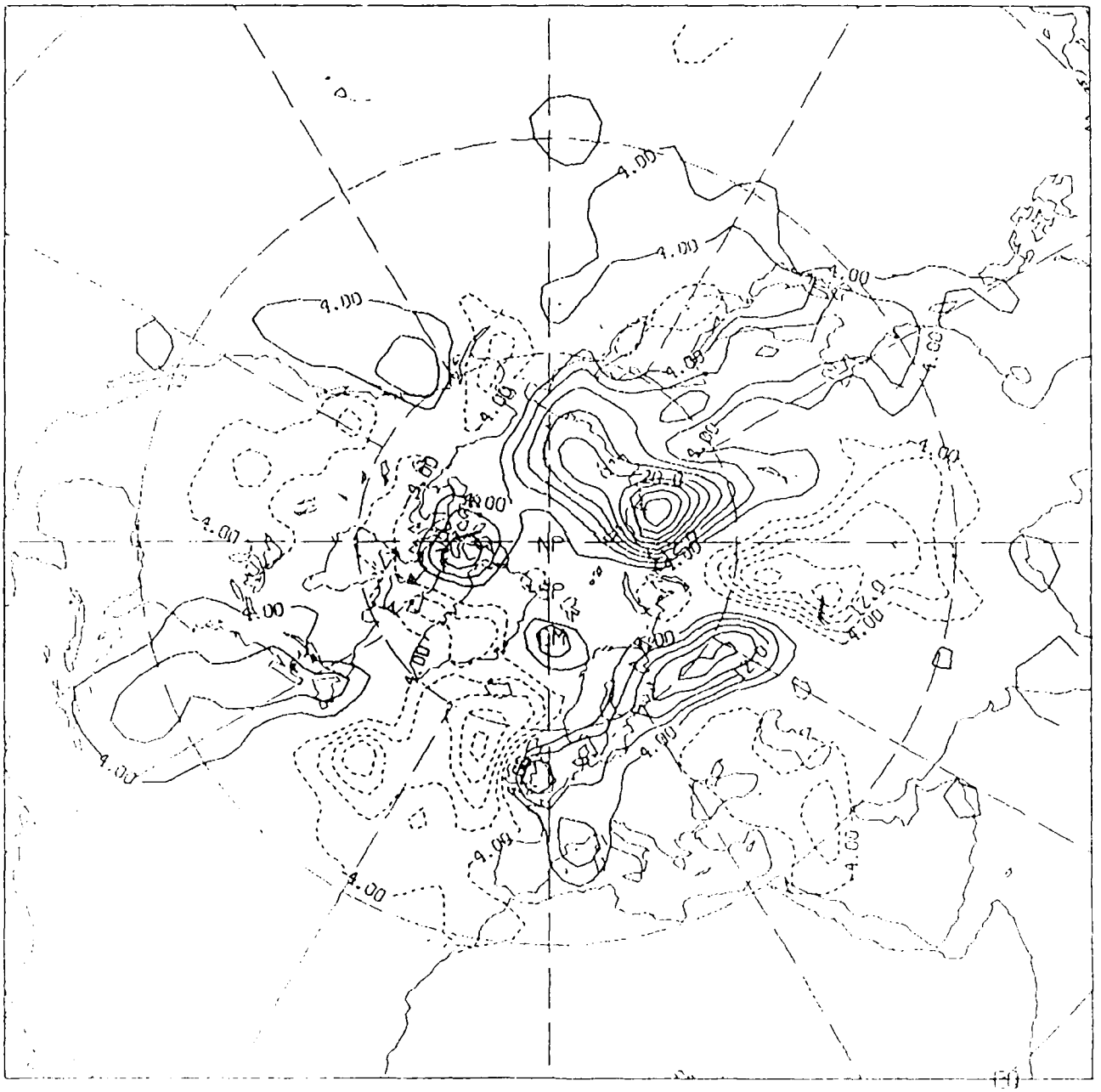

Fig. 22. The difference between NOCON and STATSAT 500 mb height analyses for the Northern Hemisphere at 00 GMT 15 February 1979.

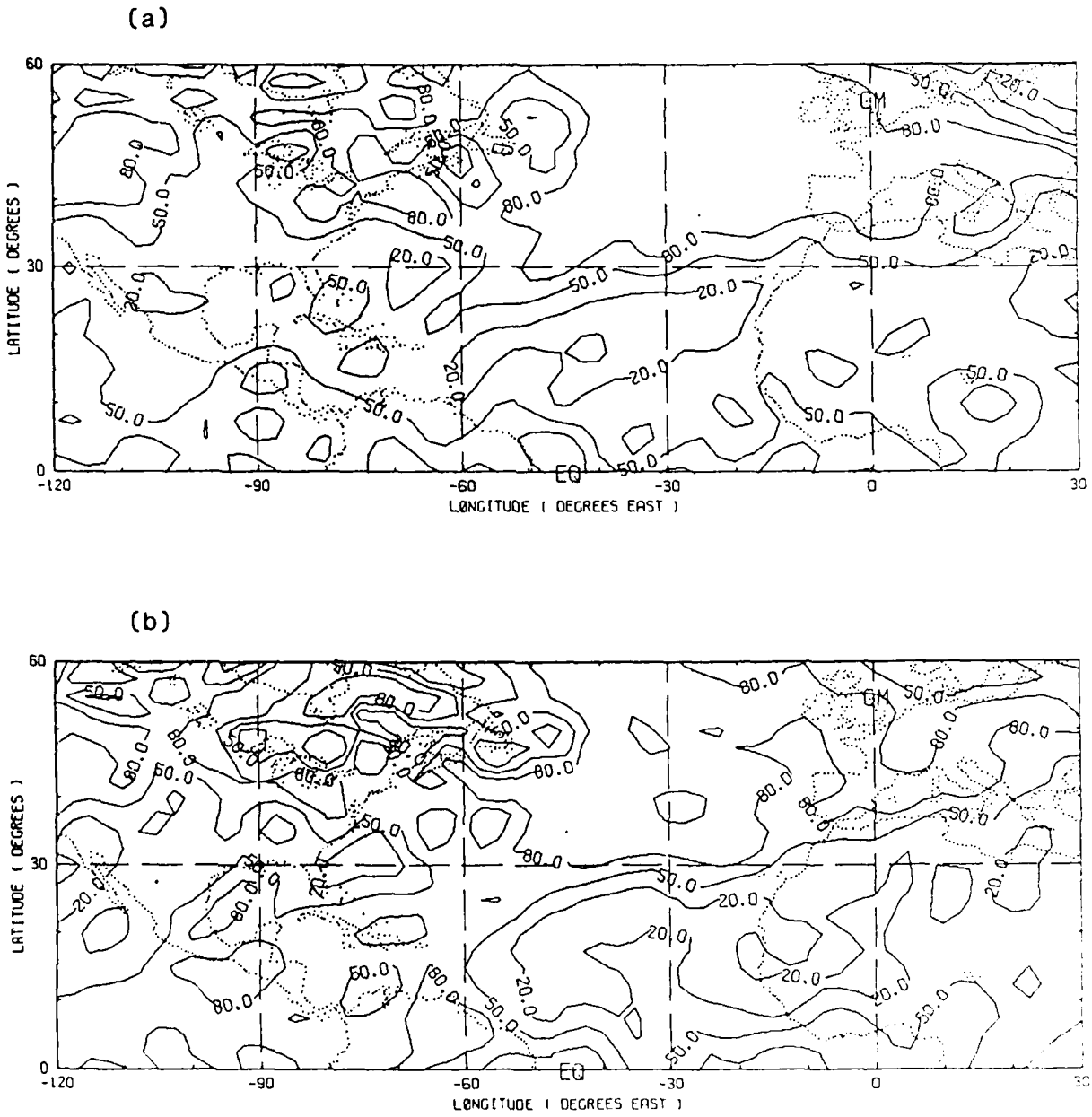

Fig. 23. The NOCON (a) and STATSAT (b) 850 mb relative humidity analyses for the North Atlantic region at 00 GMT 13 February 1979.

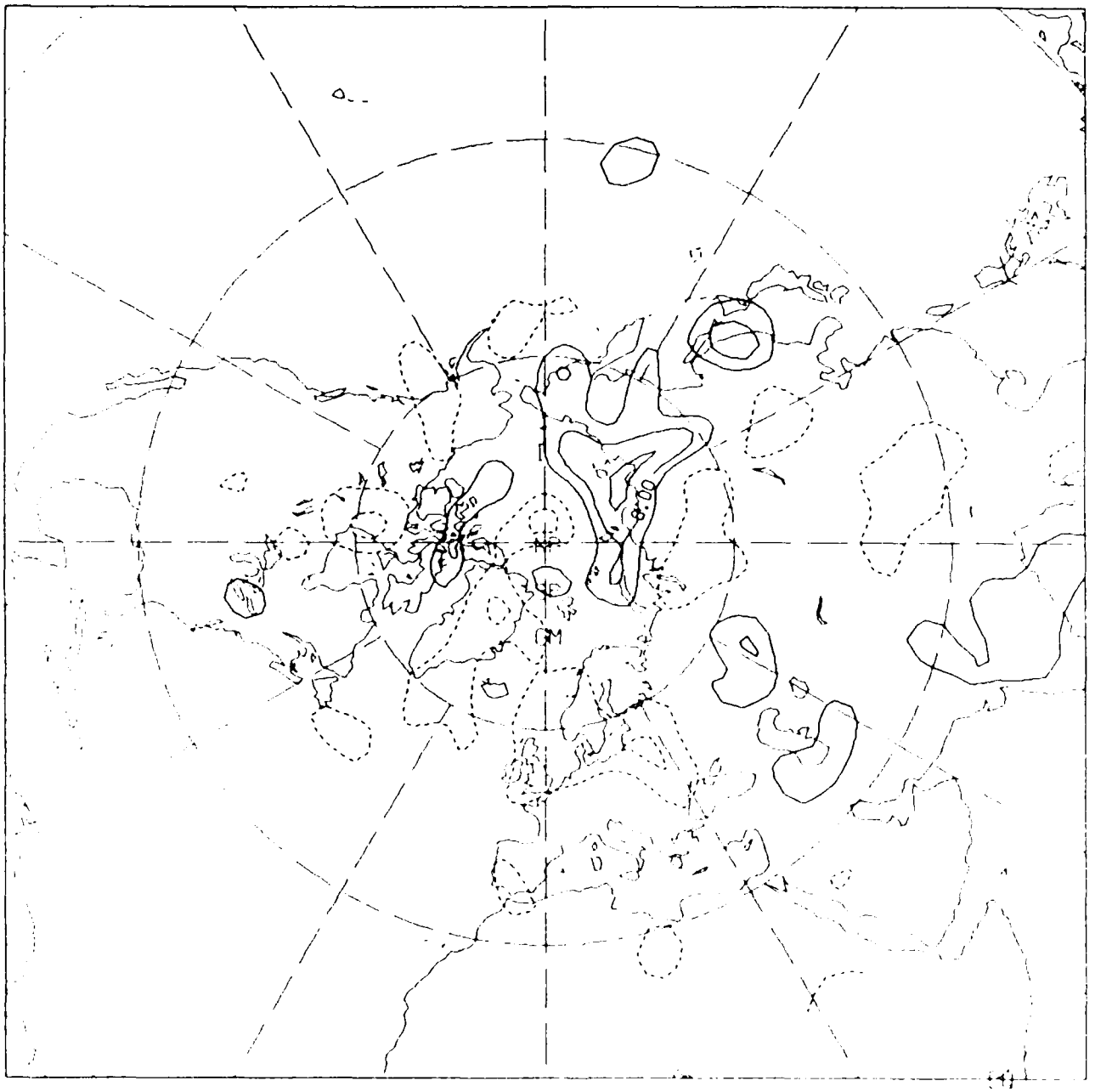

Fig. 24. The difference between NOCON and STATSAT 500 mb height analyses for the Northern Hemisphere at 00 GMT 24 June 1979.

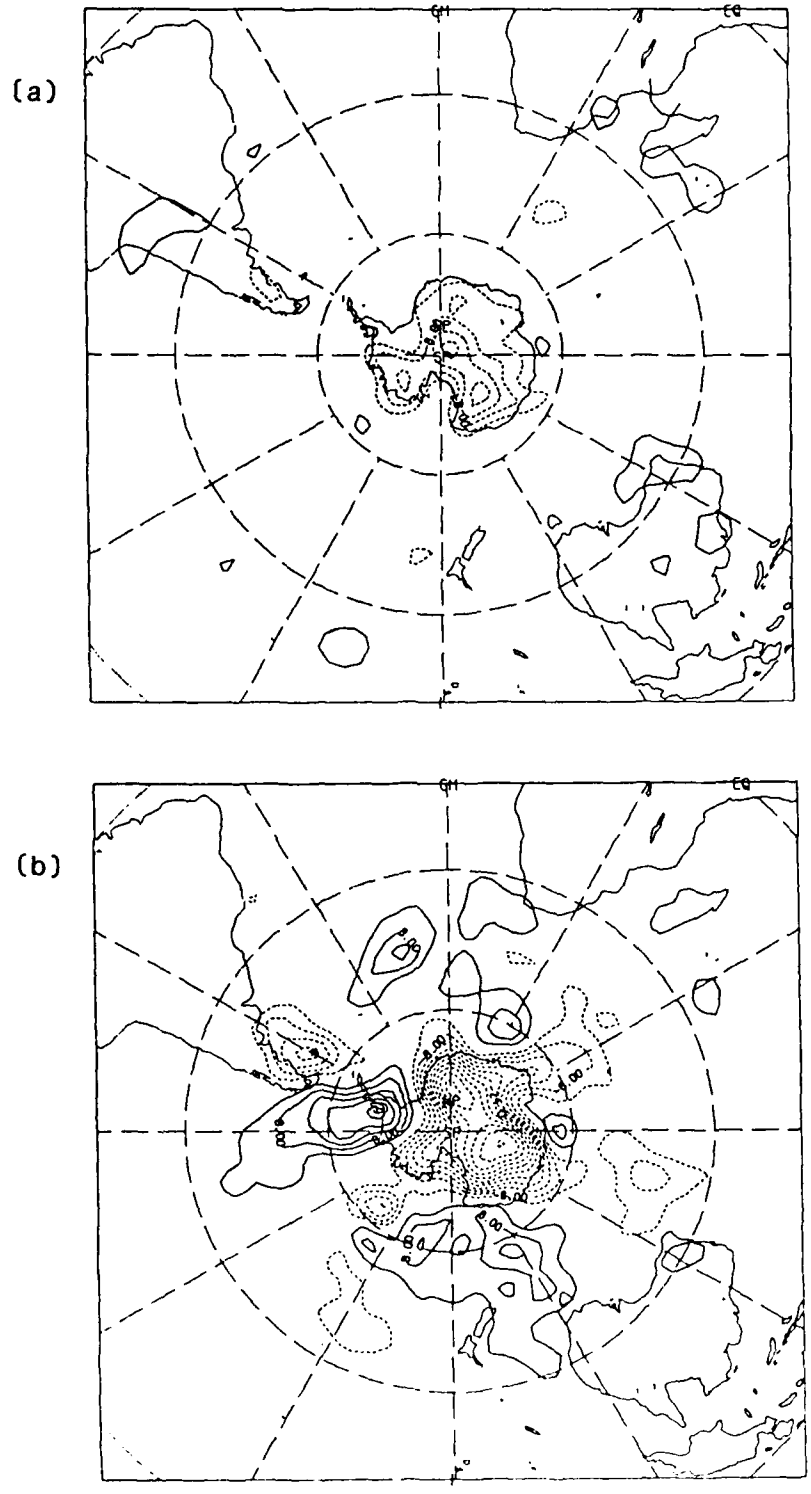

Fig. 25. The difference between NOCON and STATSAT 500 mb height analyses for the Southern Hemisphere at 00 GMT 18 June 1979 (a) and at 00 GMT 24 June 1979 (b).

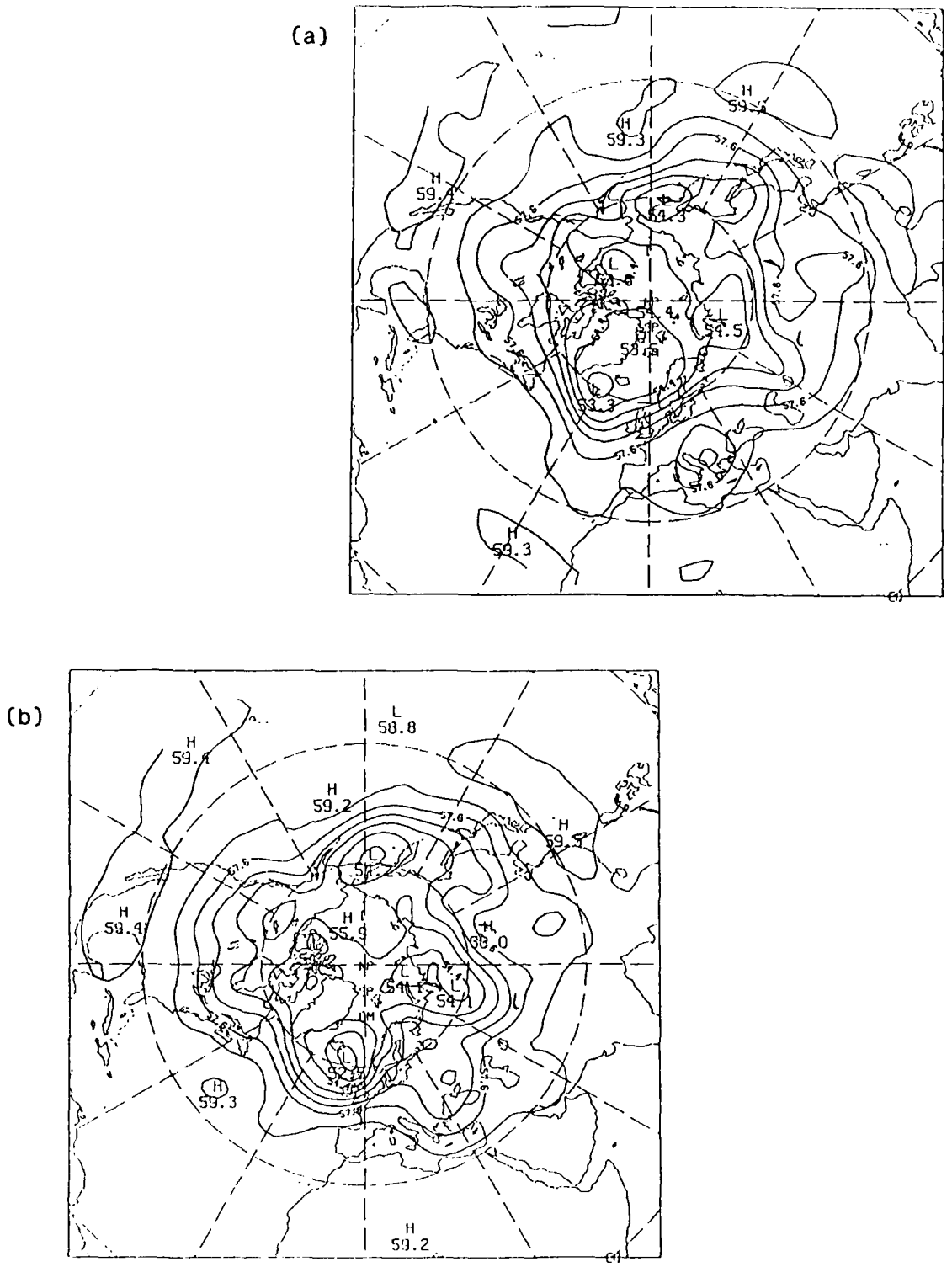

Fig. 26. The 96 h NOCON (a) and STATSAT (b) 500 mb height forecasts for the Northern Hemisphere at 00 GMT 24 June 1979.

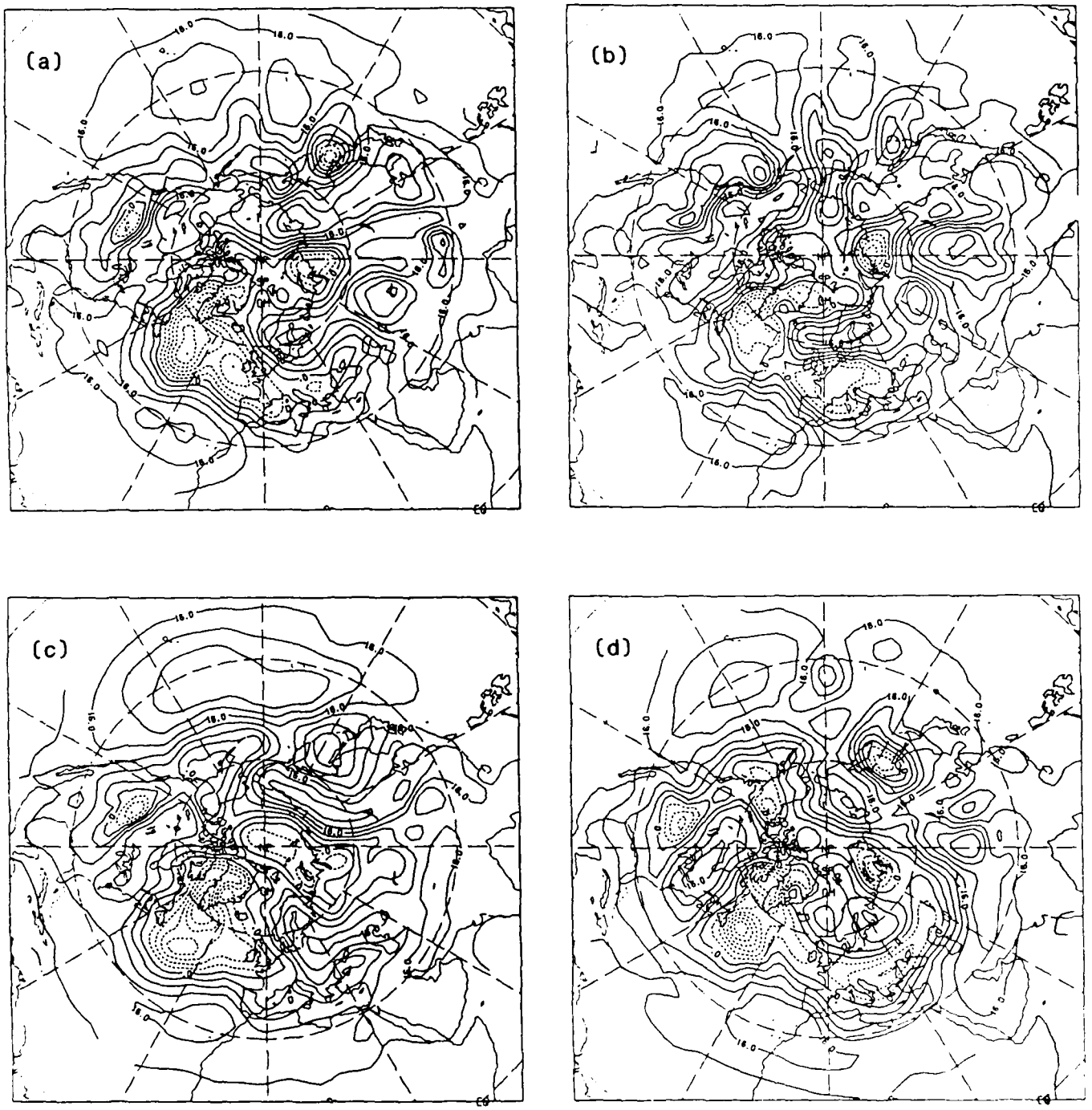

Fig. 27. The NOCON analysis (a), STATSAT analysis (b), 96 h NOCON forecast (c) and 96 h STATSAT forecast (d) of 1000 mb height for the Northern Hemisphere at 00 GMT 15 February 1979.

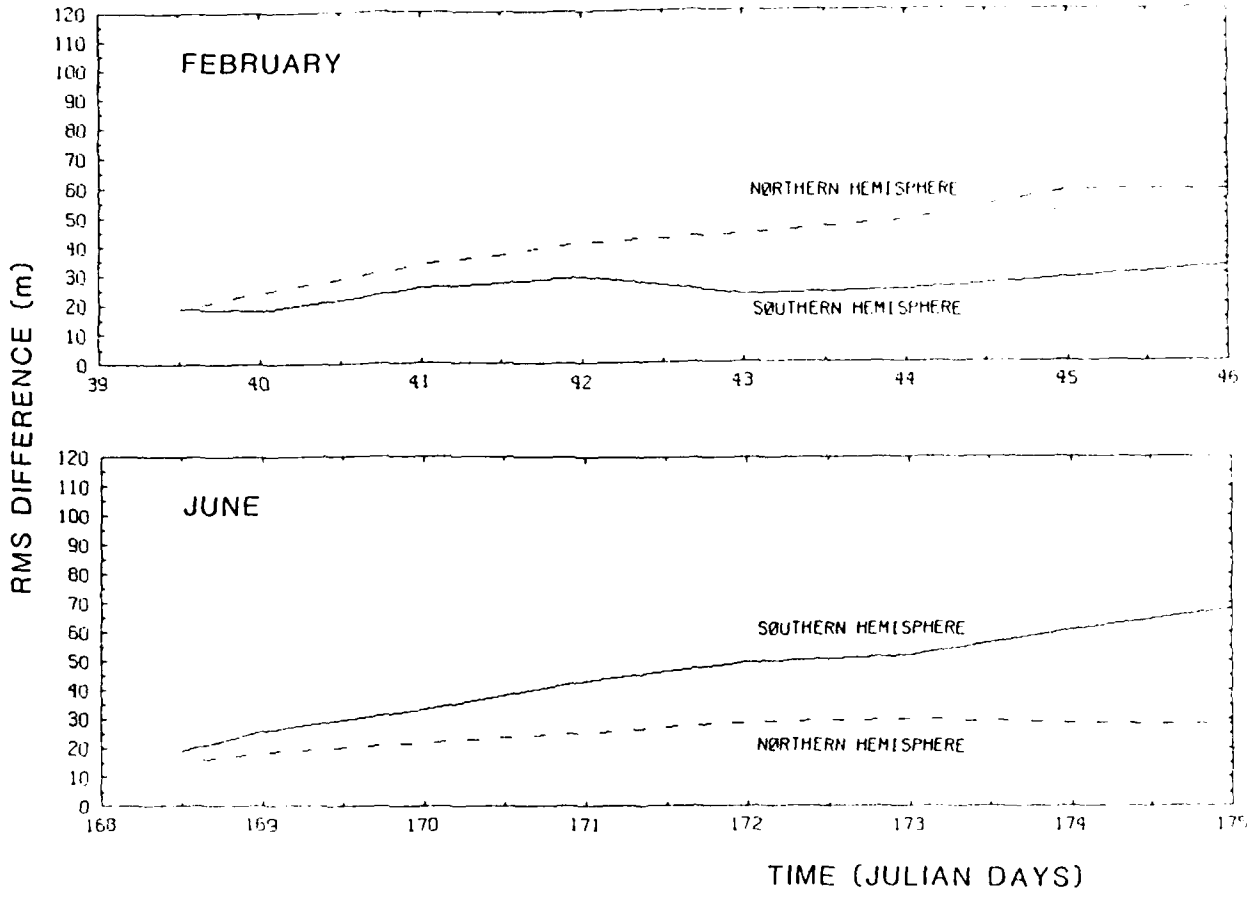

Fig. 28. Time evolution of rms differences between the NOCON and STATSAT 500 mb height analyses.

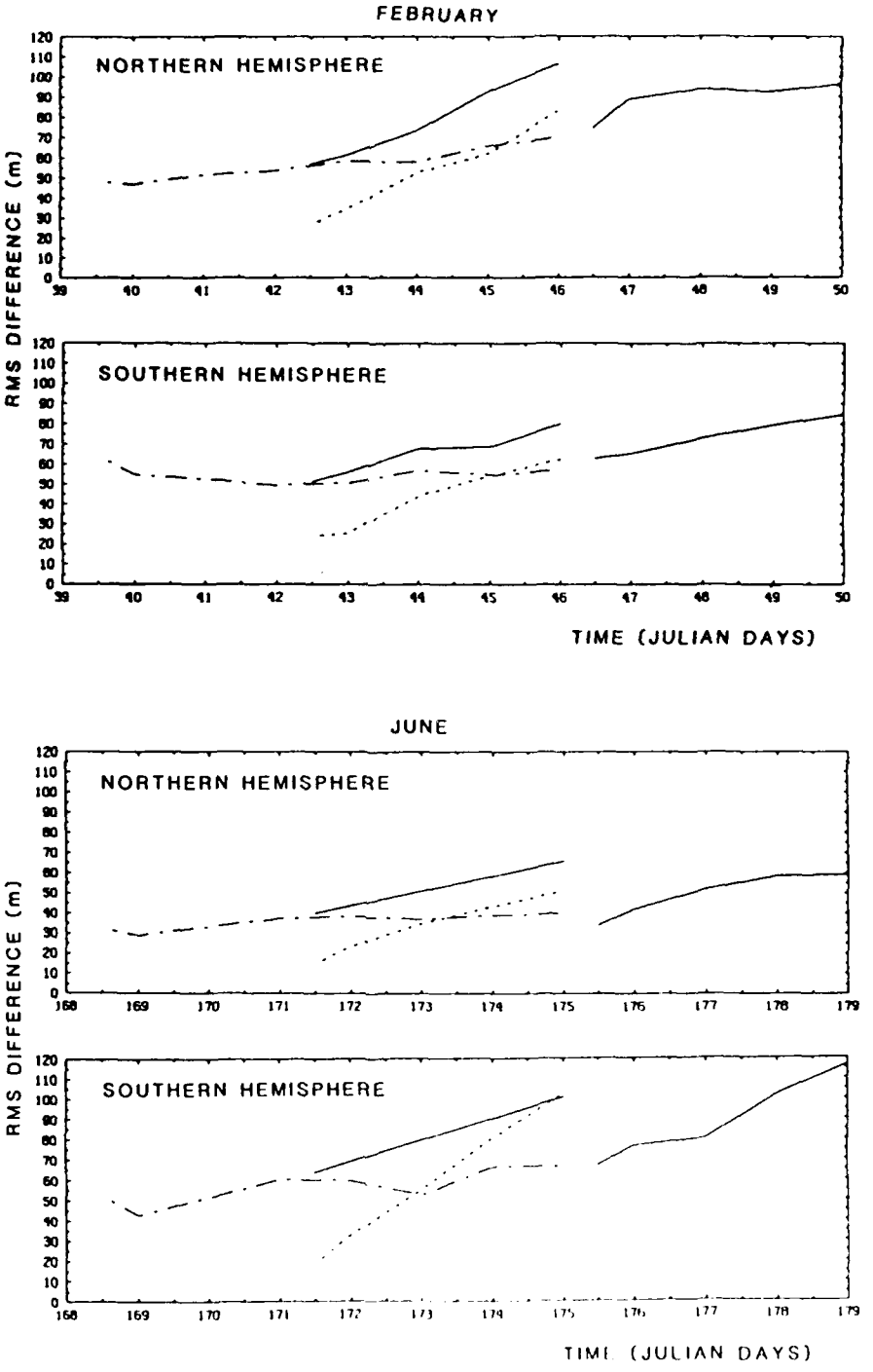

Fig. 29. Time evolution of rms differences between the 500 mb height analyses and forecasts. The comparisons shown are NOCON analysis - NMC analysis (dot-dashed line), NOCON forecast - NMC analysis (solid line) and NOCON forecast - NOCON analysis (dotted line).

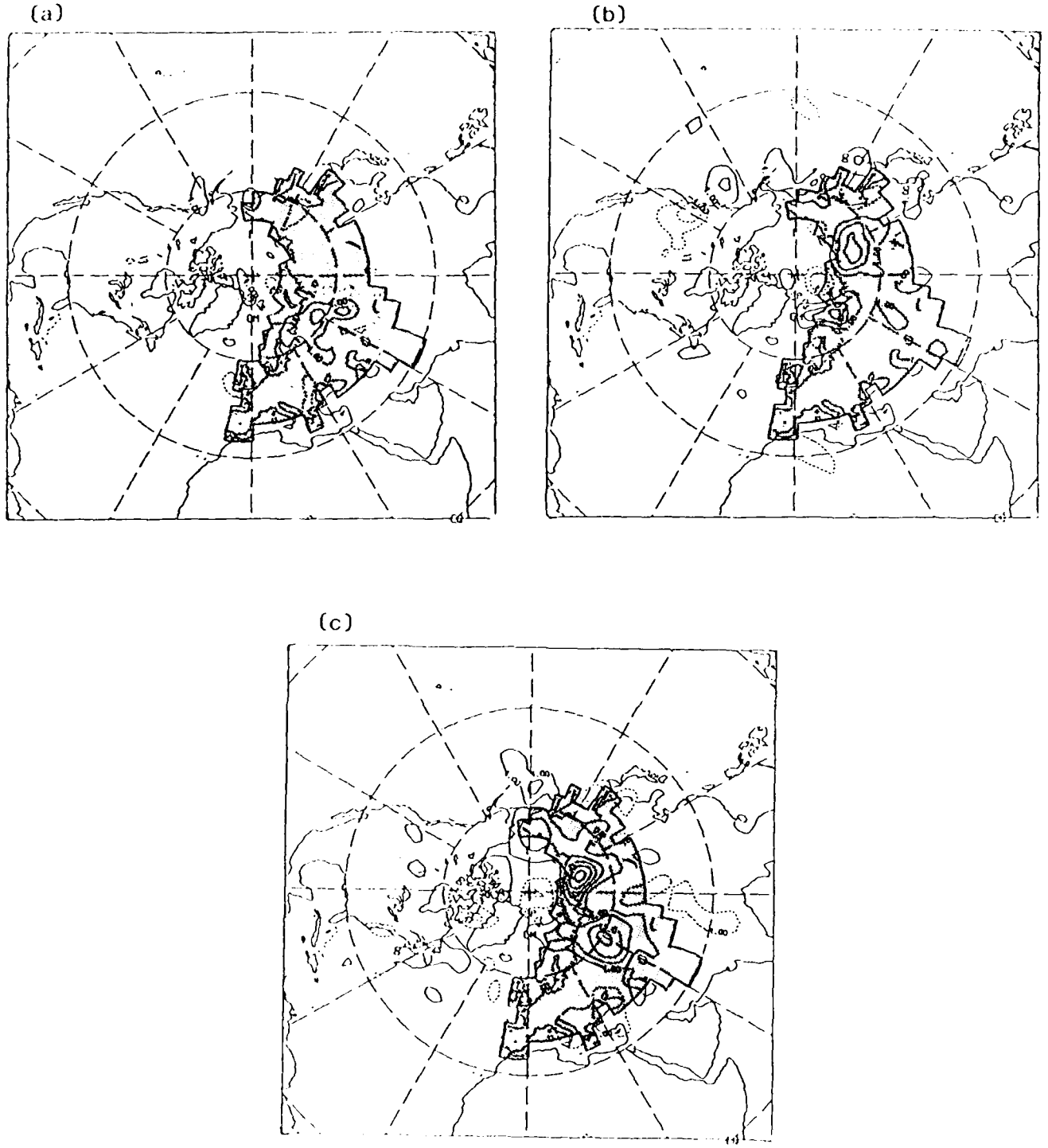

Fig. 30. The difference between NOCOR and STATSAT 500 mb height analyses for the Northern Hemisphere at 00 GMT 10 February 1979 (a), 00 GMT 12 February 1979 (b) and 00 GMT 15 February 1979 (c). The region where data was derived is shaded.

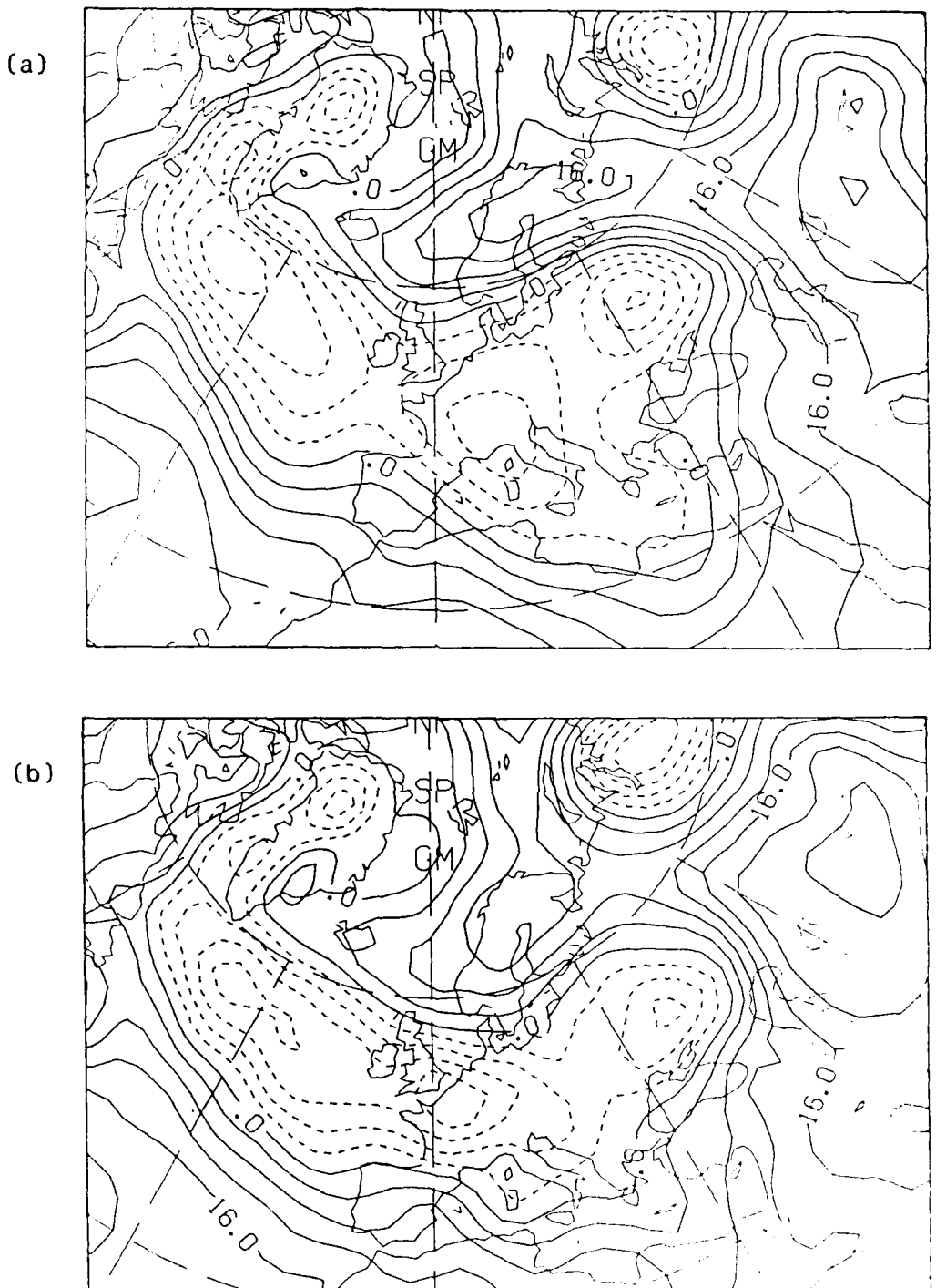

Fig. 31. The NOCOR (a) and STATSAT (b) 1000 mb height analyses for Europe at 00 GMT 14 February 1979.

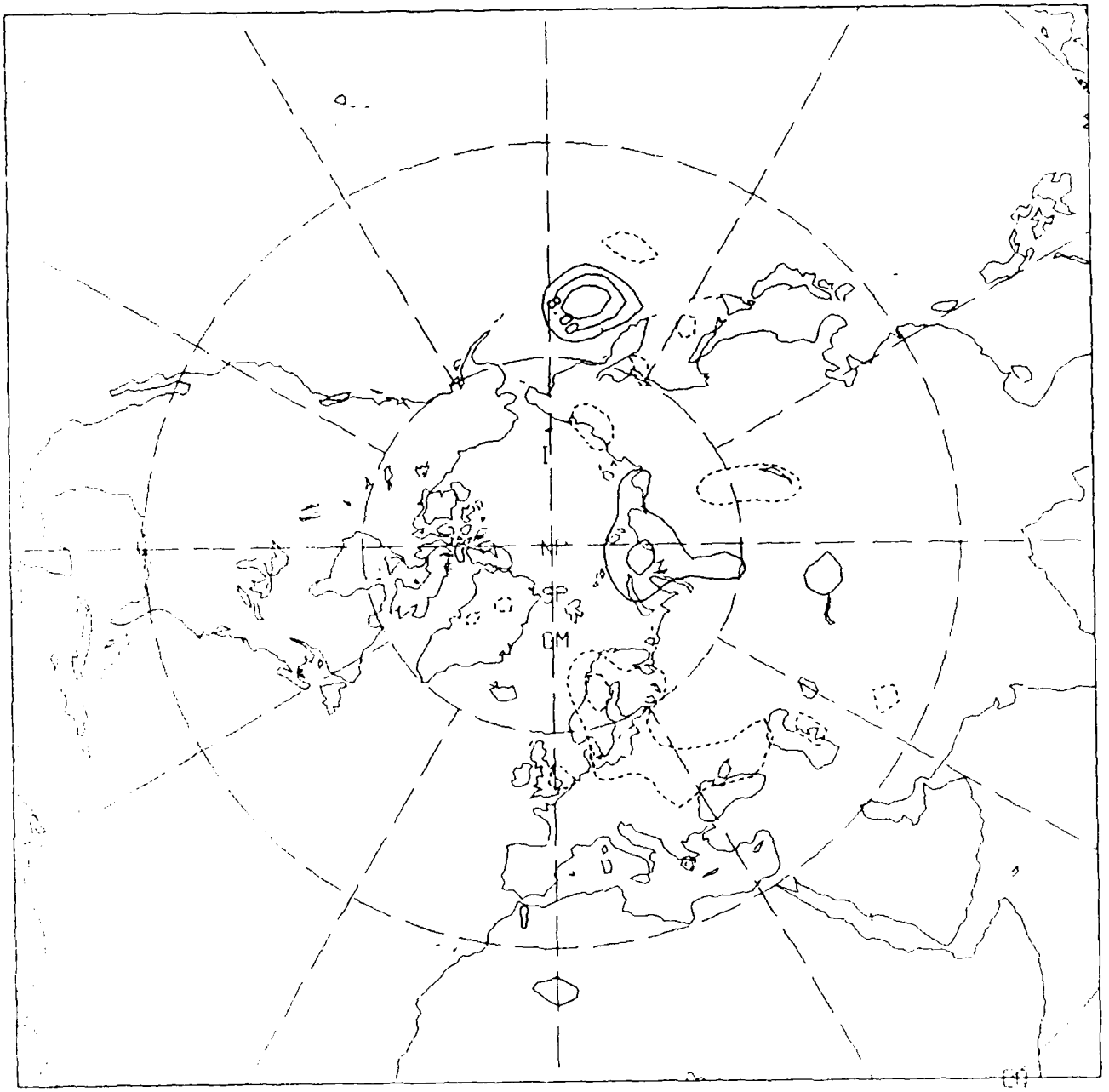

Fig. 32. The difference between NOCOR and STATSAT 1000 mb height analyses for the Northern Hemisphere at 00 GMT 22 June 1979.

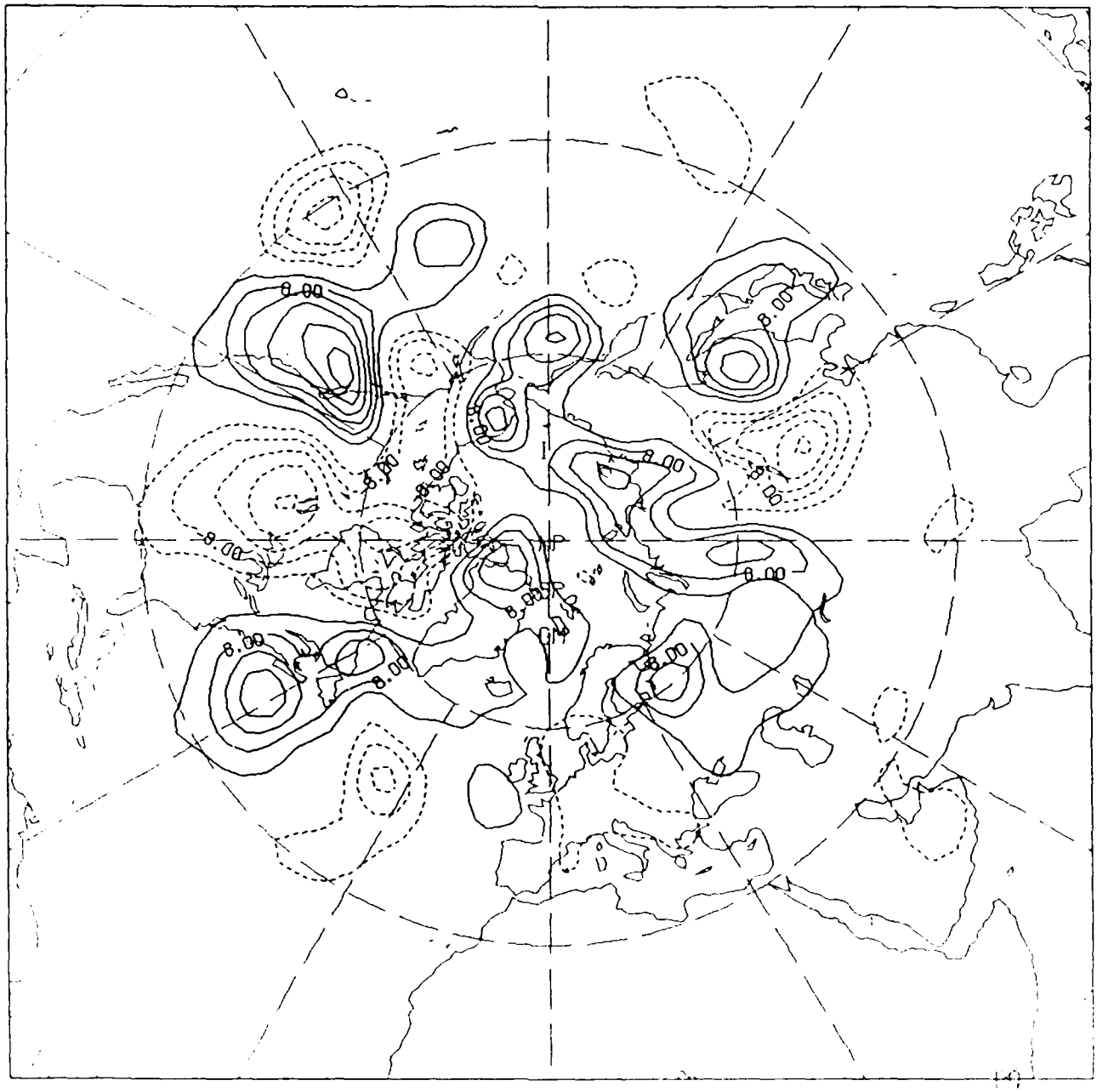

Fig. 33. The difference between NOCOR and STATSAT 72 h 500 mb height forecasts for the Northern Hemisphere at 00 GMT 14 February 1979.

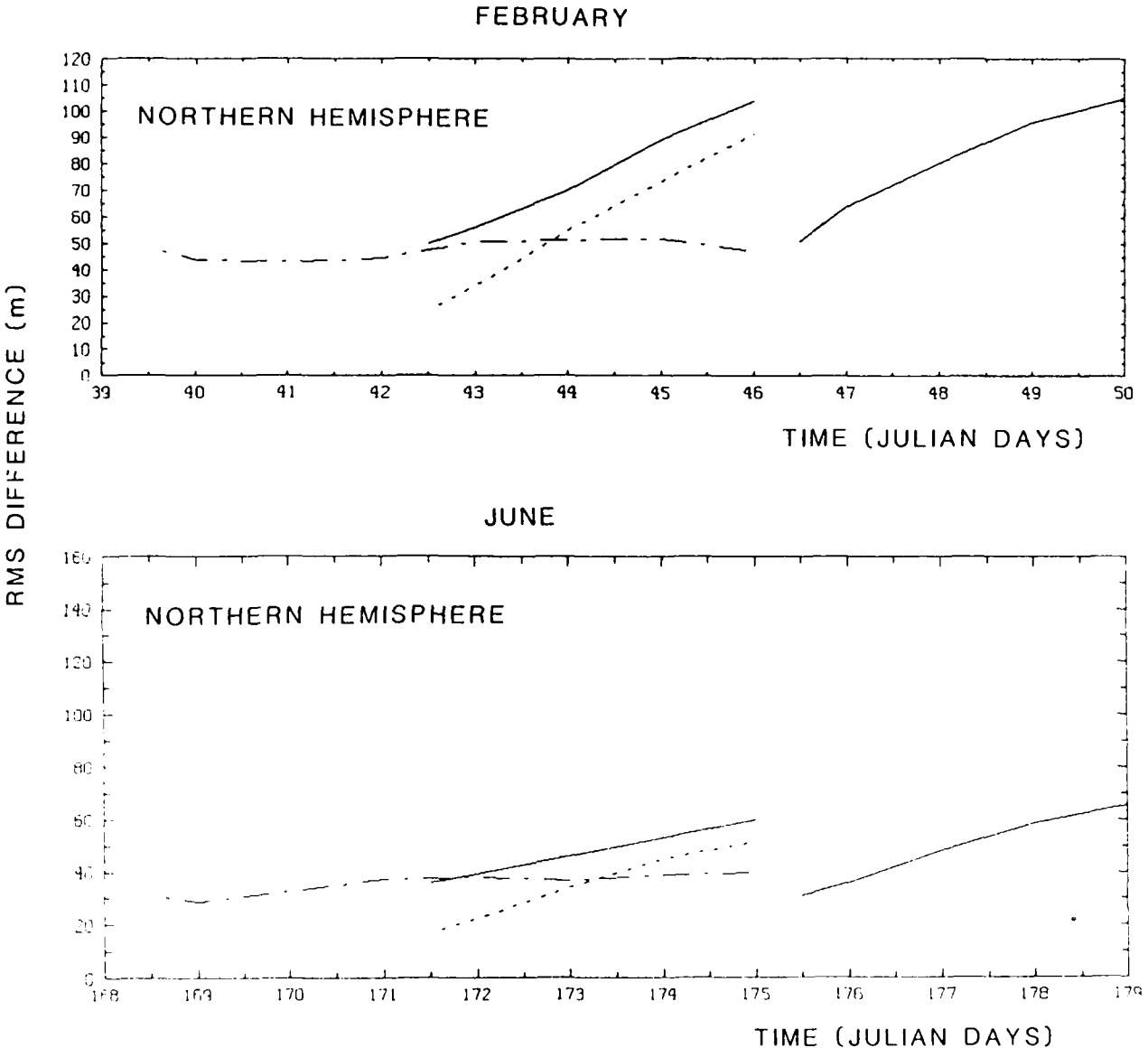

Fig. 34 Time evolution of rms differences between the 500 mb height analyses and forecasts. The comparisons shown are NOCOR analysis - NMC analysis (dot-dashed line), NOCOR forecast - NMC analysis (solid line) and NOCOR forecast - NOCOR analysis (dotted line).

END

DATE

FILMED

MARCH

1988

DTIC